Chapter-4(A)

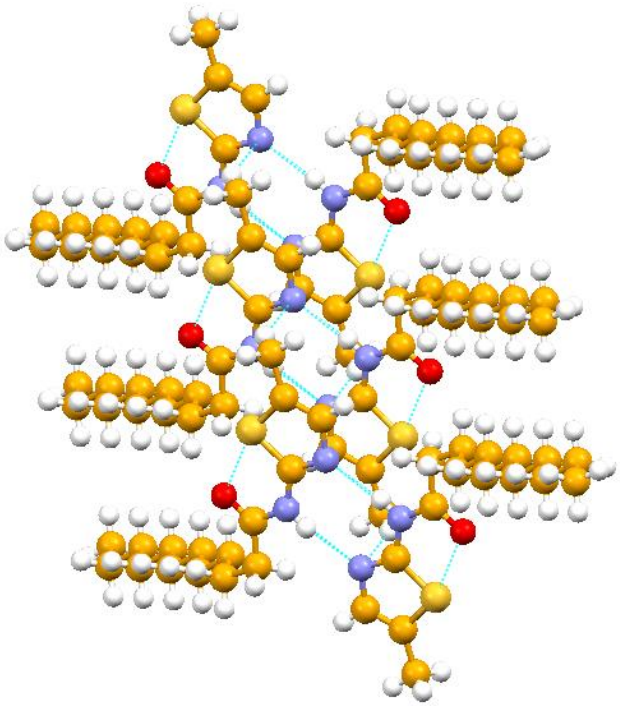

Probing the role of weaker interactions in immobilization of solvents in a novel class of Thiazole based supramolecular gelator

Published in RSC Adv., 2013, 3, 8417-8421

4.1 Introduction

Design and synthesis of new low molecular mass organic gelators (LMOGs) have shown exponential growth, which is fuelled by the desire to understand and control supramolecular assembly for tuneable property and applications.[1-6] Although, a wide variety of supramolecular gels are known but most of them are discovered by chance than design. Therefore, it is still desired to improve the understanding of the nature and cause of formation of gelator network, also known as *self-assembled fibriller networks* (SAFIN), to realize the dream of designer supramolecular gels with tailor made properties. In recent years, efforts to design new LMOGs are centred around two common strategies, namely,1) applying the concept of supramolecular synthons[7] and crystal engineering approach[8] to produce one-dimensional (1-D) hydrogen bonded network, considering that 1-D Hydrogen bonded (H-bond) network are known to favour physical gelation as compared with 2-D and 3-D H-bonded network[3], and 2) to find a robust structural moiety common to various gelling systems and test its tolerance for functional group change or substitution towards solvent gelling ability. ALS (Aromatic-linker- Steroid) based LMOG is an important class of gelators, which has been proved quite robust to various structural and substituent modification.[9] Similarly 1,3,5-triazine moiety has been shown to be an excellent scaffold for designing a new gelator.[10,11] Last chapter discussed a new series of 2-aminothiazole (and its methyl derivatives) salts and cocrystals with various dicarboxylic acids. Interestingly, one of the salt 5-methyl-2-aminothiazolium hydrogen decandioate registered its potential as hydrogelator. This inspired us to explore thiazole moity as robust structural unit for inducing gelation property. We decided to explore long chain aliphatic amide based thiazole derivatives as potent LMOGs **(Scheme 4.1)** mainly due to following reasons, i) thiazole based supramolecular gelator are not known in the literature to the best of our knowledge, ii) robust 1-D supramolecular synthon of amide functionality may lead to organogelation,[12-13] iii) to explore the role of weaker interaction such as S....S, π-π, C-H...π, C-H...O, etc. in controlling the supramolecular assembly, and iv) to establish structure-property correlation between gelling and non-gelling behaviour of various thiazole derivatives.

4.2. Experimental

4.2.1 Materials and physical measurements

4.2.1.1 Materials

2-Amino thiazole (97%), 2-Amino-4-methylethiazole (98%), 2-Amino-5- methyl-thiazole (98%),Tetradecanoic acid(99%) (All from Aldrich) were used as received. The other chemicals were of the highest commercial grade available and were used without further purification. The liquids used for the preparation of gels were reagent grade. All solvents used in the synthesis were purified, dried and distilled as required.

4.2.1.2 FT-IR spectroscopy

FTIR Spectra were recorded on a Perkin Elmer –RX FT-IR instrument. Solid samples were recorded as an intimate mixture with powdered KBr.

4.2.1.3 ^{1}H-NMR Experiments

The ^{1}H- NMR spectra were measured by using a Bruker AVANCE, 400MH$_Z$ NMR instrument with TMS as internal standard.

4.2.1.4 Scanning Electron Microscopic Study

Morphologies of all reported gel materials were investigated using scanning electron microscopy (SEM). For SEM study, the gel materials were dried to give xerogel, and then the micrographs were taken in a SEM apparatus (JEOL JSM5610 LV microscope).

4.2.1.5 Powder X-ray Diffraction Study

The X-Ray diffraction patterns were recorded for compound **3** in solid state and xerogel obtained by evaporating methanol using Rigaku powder X-ray diffractometer model Multiflex 2kW. The typical width is 0.250° and minimum height is 200 cps.

4.2.1.6 Single Crystal X-ray studies

Single crystal X-ray study of compounds **1** and **2** was carried out on Single Crystal X-ray diffractometer (Xcalibur, EOS, Gemini diffractometer) at 298 K. Crystals of **3** was obtained from methanol in a slow evaporative condition at room temperature. Diffraction data for **3** was collected using MoKα (λ=0.7107Å) radiation on a SMART APEX diffractometer equipped with CCD area detector. All structures were solved and refined using the Olex2 software[14] and ShelXL[15] refinement package. Graphics were generated using MERCURY 3.3.

All structures are solved by direct methods and refined in a routine manner. In all cases, nonhydrogen atoms are treated anisotropically. Whenever possible, the hydrogen atoms are located on a difference Fourier map and refined. In other cases, the hydrogen atoms are geometrically fixed.

4.2.1.7 Gelation Test

A weighted amount of potential gelator (1wt %) and a measured volume of selected pure organic solvent were placed into a test tube and the system was heated in an oil or water bath until all solid materials were dissolved. The solution was cooled to room temperature and finally, the test tube was turned upside down to observe if the solution inside could still flow. A positive test is obtained if the flow test is negative. Systems in which only solution remained until the end of the tests are referred as solution (S). Systems that are clear solutions when they are hot but precipitation or crystallization occurs when they are cooled down to room temperature are denoted by P (precipitation) and C (crystallization), respectively.

4.2.1.8 T_{gel} Measurement

Temperatures of gel-to-sol transition (T_{gel}) were determined by using a conventional "falling ball" method. In this test, a small glass ball (63mg) was carefully placed on the top of the gel to be tested, which was produced in a test tube. The tube was slowly heated in a thermostated oil bath until the ball fell to the bottom of the test tube. The temperature at which the ball reaches at the bottom of test tube is taken as T_{gel} of that system.

4.2.2 General Synthesis methodology

Oxalyl chloride (2ml, 20 mmol) was added slowly to a stirred solution of tetradecanoic acid (2 mmol) in dry dichloromethane(10mL) under a nitrogen atmosphere, and stirring was continued under a nitrogen atmosphere for 12 h. Excess oxalyl chloride and solvent were then removed by distillation under reduced pressure. The acid chloride so obtained was dissolved in dry dichloromethane (10 mL) and added to the amine (2 mmol) in triethylamine (0.3ml, 2.15mmol). The mixture was stirred under a nitrogen atmosphere for overnight. The reaction mixture then added to dilute hydrochloric acid (5%), and extracted with chloroform. The product residue after removing chloroform was purified by repeated recrystalization from ethyl acetate/pet ether mixture.

4.2.3 Analytical data

N-(thiazol-2-yl)tetradecanamide **(1)**: Yield 72%, m.p. 140 °C, ^{1}HNMR (400MHz, $CDCl_3$, TMS); δ 7.458 (d,1H; CH), 7.026 (d, 1H; CH), 2.586-2.547 (t, 2H; CH_2), 1.808-1.771 (m, 2H, CH_2), 1.406 -1.368 (m, 20H, CH_2), 0.911-0.877 (t, 3H; CH_3).

MS (EI): m/z 310.16 $[M]^+$.

FT-IR(KBr): 3271,3175, 2917, 1685, 1581, 1467, 1380, 1382, 1284, 1169, 1066, 958, 873, 777, 718, 626, 520, 457 cm^{-1}.

N-(4-methylthiazol-2-yl)tetradecanamide **(2):**Yield 69%, m.p.60°C, ^{1}HNMR (400 MHz, $CDCl_3$, TMS): δ 6.553 (s,1H;CH), 2.540-2.419 (t,2H,CH_2), 2.388 (s,3H; CH_3), 1.789-1.693 (m,2H;CH_2), 1.373-1.266 (m,20H;CH_2), 0.922-0.912 (t,3H;CH_3). MS (EI): m/z 324.34 $[M]^+$.

FT-IR(KBr): 3541, 3281, 2916, 1988, 1683, 1550, 1467, 1408, 1376, 1310, 1263, 1176,1011,987,765,423.

N-(5-methylthiazol-2-yl)tetradecanamide **(3):**Yield 80%, m.p. 125°C,^{1}HNMR(400 MH_Z, $CDCl_3$, TMS): δ 7.065 (s,1H;CH), 2.537 –2.499 (t,2H; CH_2), 2.433 (s,3H; CH_3),1.809-1.735 (m,2H;CH_2), 1.400-1.26 (m,20H;CH_2), 0.912- 0.877 (t,3H; CH_3). MS (EI): m/z 324.18$[M]^+$.

FT-IR(KBr): 3283, 3180, 2918, 2849, 1698, 1587, 1462, 410, 1379, 1312, 1280, 1188, 1165, 1110, 1032, 993, 953, 835, 786, 672, 527, 458 cm^{-1}.

4.3 Results and discussion

A new class of thiazole based amide derivatives was synthesized by reacting acid chloride of Tetradecane carboxylic acid with thiazole derivatives **(Scheme4.1)** using a modified synthetic procedure.[16] All synthesized compounds were characterized by FT-IR, ^{1}H-NMR and MS analysis.

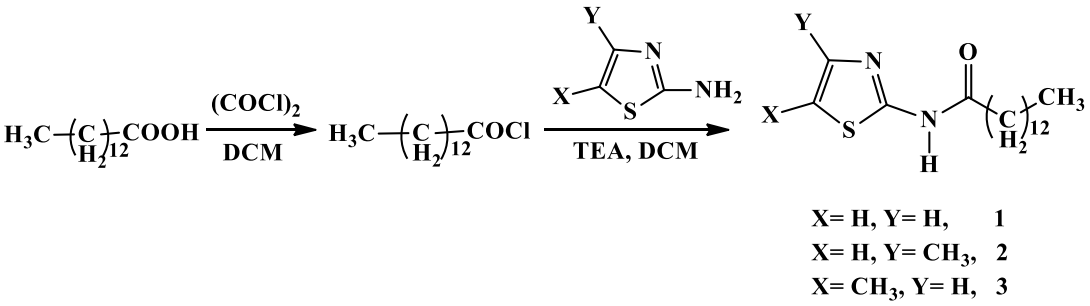

Scheme 4.1 List of compounds synthesized.

Unsubstitued thiazole amide derivative **1** was examined for gelation behaviour towards polar and non-polar solvents **(Table 4.1)**. Surprisingly, **1** showed good gelation property towards various polar and non-polar solvent with minimum gelation concentration (MGC) ranging between 0.70 (wt%, w/v) for n-octadecane to 2.80 (wt %, w/v) for n-pentanol.

In order to improve the gelation behaviour towards various solvents we followed a simple strategy of substitution of thiazole ring. The functional group attached with thiazole moiety may provide additional sites for hydrogen bonding or may strengthen existing hydrogen bonding through inductive effect in supramolecular assembly. 4-methyl and 5- methyl substituted thiazole moiety was used for synthesizing new series of amide based compounds.

To our surprise 5-methyl-2-tetradecanamidothiazole, **3** turned out to be excellent organogelator **(Figure 4.1)**, whereas 4-methyl-2- tetradecanamidothiazole **2**, found to be incapable of immobilizing any solvent used in the present study **(Scheme 4.2)**. Compound **3** had shown a super gelation property (MGC <1% w/v) towards various alcohols such as ethanol, butanol, propanol, etc. and reasonably good gelation behaviour towards non-polar solvent such as n-octadecane (MGC= 1.16 % w/v) **(Table 4.1)**.

Table 4.1 Gelation studies of compounds 1-3 in various solvents

	1	2	3
Methanol	G (1.86)	S	G (0.65)
Ethanol	G (2.16)	S	G (0.80)
n-Pentanol	G (2.80)	S	G (2.12)
n-Heptanol	S	S	G (3.83)
Water	P	P	P
THF	S	S	S
Iso octane	G (2.42)	S	G (0.90)
Xylene	C	S	C
Cyclohexane	G (2.40)	P	G (3.17)
n-octadecane	G (0.70)	P	G (1.16)

G=gel, P=precipitate, C=crystals, S=solution, values in the parenthesis represent MGC (minimum gelator concentration) in wt %(g/100mL of solvent).

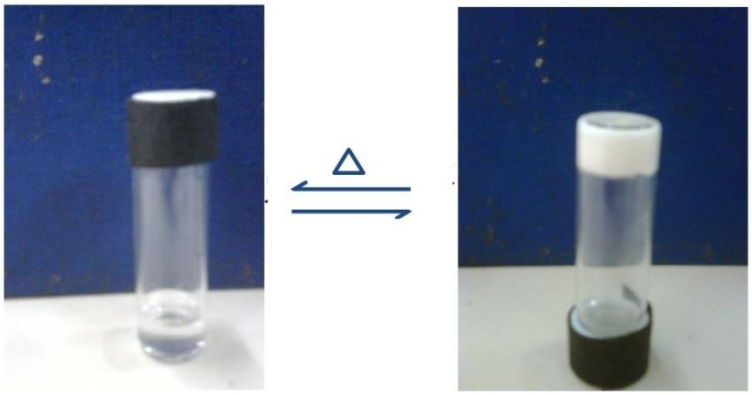

Figure 4.1 Photographic image of sol-gel transition of **3** in methanol.

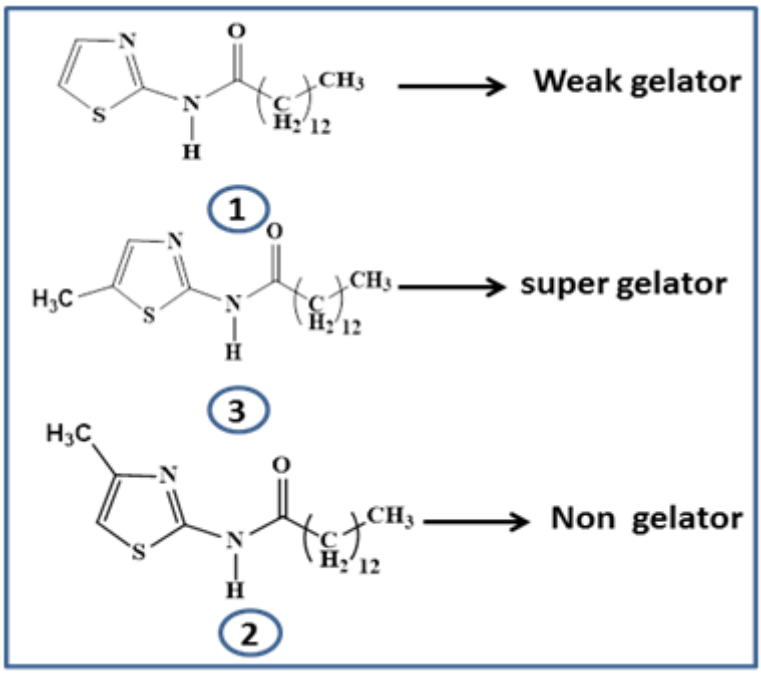

Scheme 4.2 Gelation behaviour of compounds 1-3.

The gel-to-sol transition temperature (T_{gel}) of both compound 1 and 3 was found to be well above the boiling point of methanol **(Figure 4.2)** suggesting better thermal stability of the gel network.

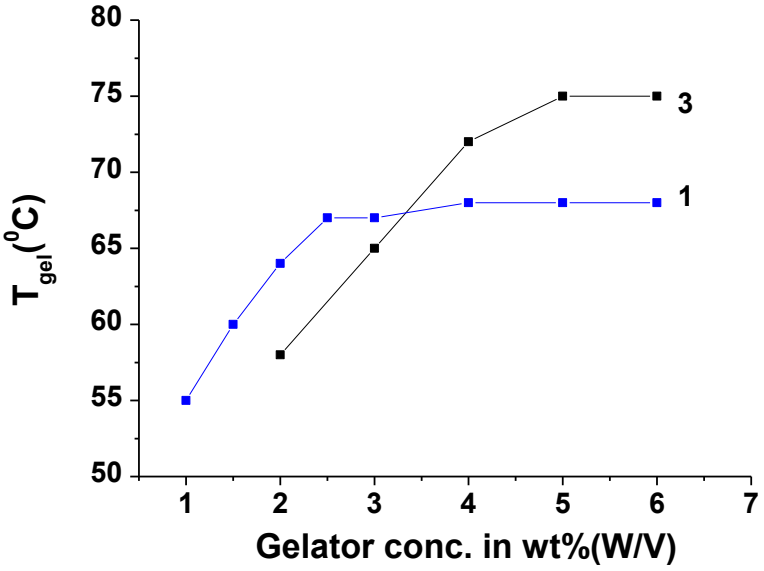

Figure 4.2 T_{gel} versus concentration plot of the gelators **1** and **3** in methanol.

To study the morphology of gelator fibres a detailed SEM analysis was carried out on xerogel (dried gel) of **1** and **3** obtained from methanol gel **(Figure 4.3)**. The xerogel of **1** showed a well-defined independent assembly of tubular morphology. Presumably, such loose collections of crystalline tubes immobilize solvents, resulting in a weak gel.Whereas; SEM image of xerogel of **3** displayed highly crossed linked intertwined fibres. Understandably, highly cross linked network of fibres would be capable of hardening a solvent easily than a bundle of tubes/tapes, which lacks a junction point and/ or cross linking.

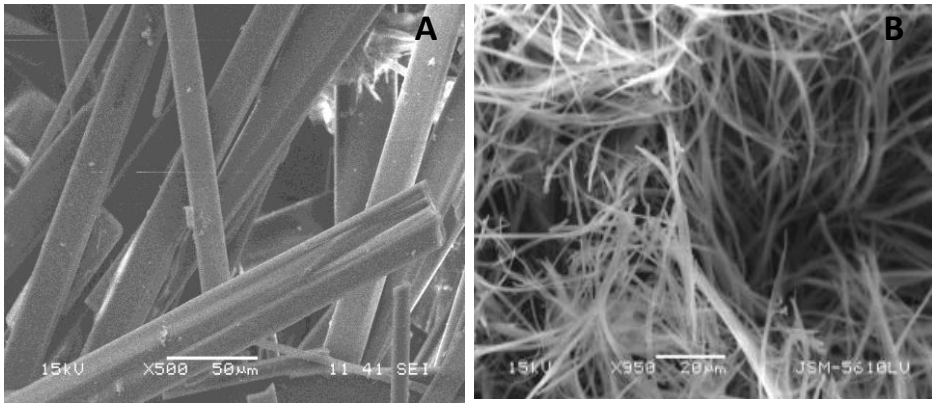

Figure 4.3 SEM images of xerogel of A) **1** and B) **3** from methanol.

FT-IR study of gelling molecules in various states namely, gel, solution and solid state were carried out to ascertain any variation in H-bond pattern in different states. Strong IR absorption peak for amides C=O stretching vibration was observed for **3** at 1693 (cyclohexane solution), 1697(cyclohexane gel),1698 cm^{-1} (Solid) and for the gelator **1** at 1687(cyclohexane solution), 1685 (cyclohexane gel),1685 cm^{-1} (solid), respectively **(Figure 4.4)**. Moreover, no significant change in wave number for N-H bending vibration (amide II band) was observed in various states namely, solid and gel for **3** from 1587 and 1589 cm^{-1} (cyclohexane), and for **1**from 1581 and 1589 cm^{-1} (cyclohexane), respectively. The IR study of gelator molecules in various states definitely suggests the retention of H-bond pattern involving the C=O and N-H bonds of amides in all the different states.

Temperature variation ^{1}H NMR study is frequently being employed to ascertain the supramolecular assembly governed by H-bonding and π-π stacking in sol or gel state. Significant changes in the chemical shift with changes in temperature (change in state) undoubtedly suggest a change in the hydrogen bonding pattern or role of π-π stacking in gelation process.[17]

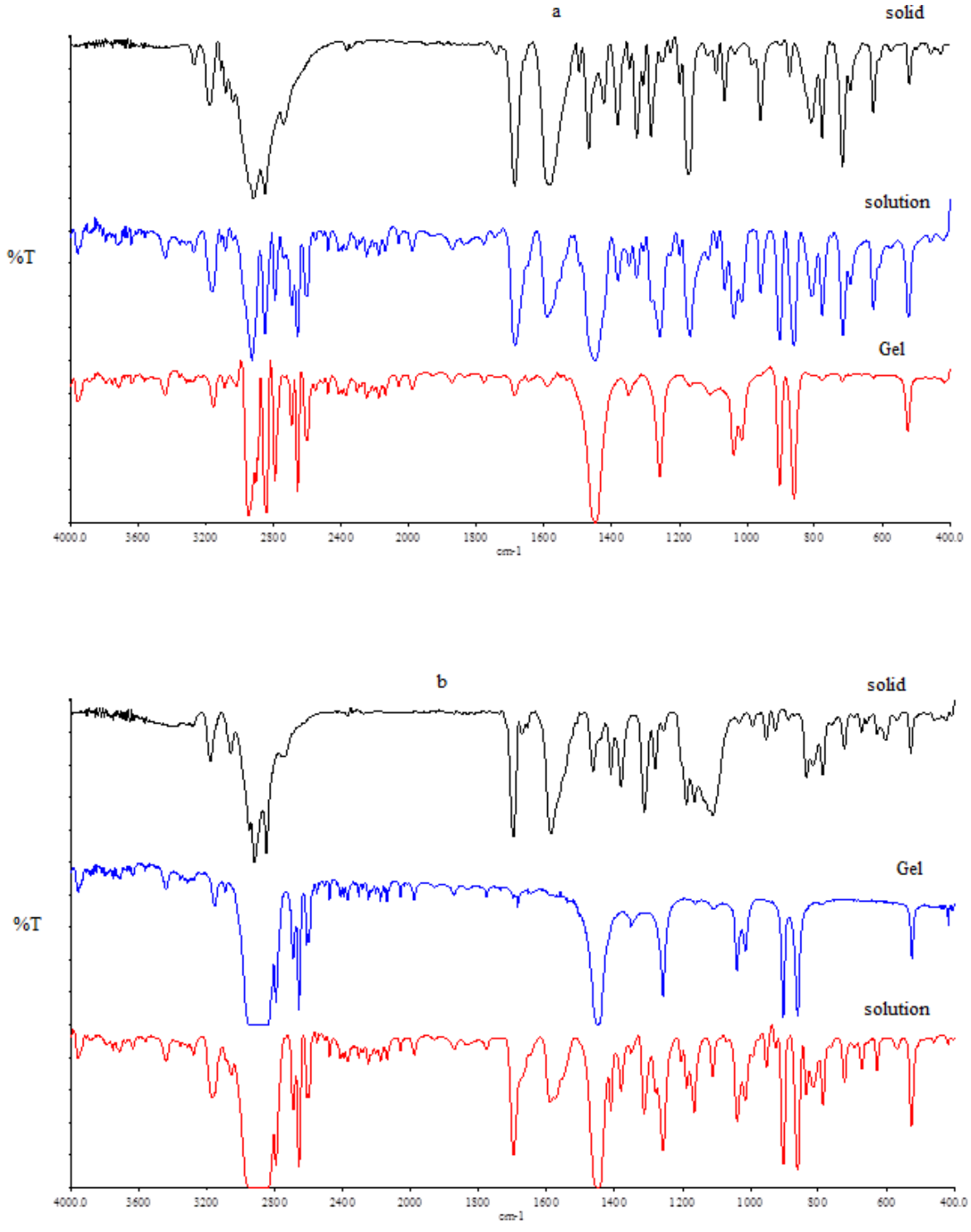

Figure 4.4 IR spetra of compounds (a) **1** and (b) **3** in cyclohexane.

A detailed variable temperature ^{1}H NMR (VT-NMR) study of gel-to-sol transition of **3** in CD_3OD was carried in the temperature range from 30° C (gel) to 70 °C (sol) by a

systematic increase of temperature by 10 °C. All protons of **3** showed a negligible change in chemical shift while going from the gel (30°C) to sol (70°C) suggesting no change in the hydrogen bonding pattern of amide group and π-π stacking of the thiazole ring **(Figure 4.5 and 4.6)**. Similarly, the weak gelling molecule **1**, i.e. 2-tetradecanamidothiazole, showed a minor chemical shift in all protons with changes in state from gel-to-sol. Therefore, IR and VT-NMR studies establish without doubt the stability of SAFIN of **1** and **3** in solid, liquid and gel states.

The variable temperature (VT) ^{1}H-NMR of non-gelling compound, **2** in CD_3OD was also carried out to understand the probable reasons for its non-gelation towards solvents used for present study. Surprisingly, the proton at position 5 of the thiazole ring showed a significant shift **(Figure 4.7)**, suggesting a probable π-π or C-H...π interaction between thiazole rings, which was missing in gelling compounds (**1** and **3**) studied using VT-NMR **(Figure 4.5 and 4.6)**. Non-gelling property of compound **2** may be attributed to additional stability provided by π-π or C-H...π interaction between thiazole rings. Furthermore, no considerable change in chemical shift of any another proton suggest no change in H-bonding network of **2** with change in temperature.

The present study clearly suggests the position of a methyl group attached to thiazole moiety is decisive in bringing about the gelation or non-gelation property in this class of gelator. As FT-IR and VT-NMR proved futile to decipher the role of methyl group on organogelation, efforts were dedicated towards growing single crystals of gelator molecules. Fortunately, our effort had yielded both the gelator crystals **1** and **3** and the non-gelator **2**. Single crystals of **1** and **3** were grown from methanol, which is also a gelling solvent, suggesting a delicate balance between the metastable gel phase and crystalline state. Surprisingly, all crystals crystallize out in a space group Monoclinic P 2_1/c, showing one molecule in the asymmetric unit (crystallographic parameters- **Table 4.2**).

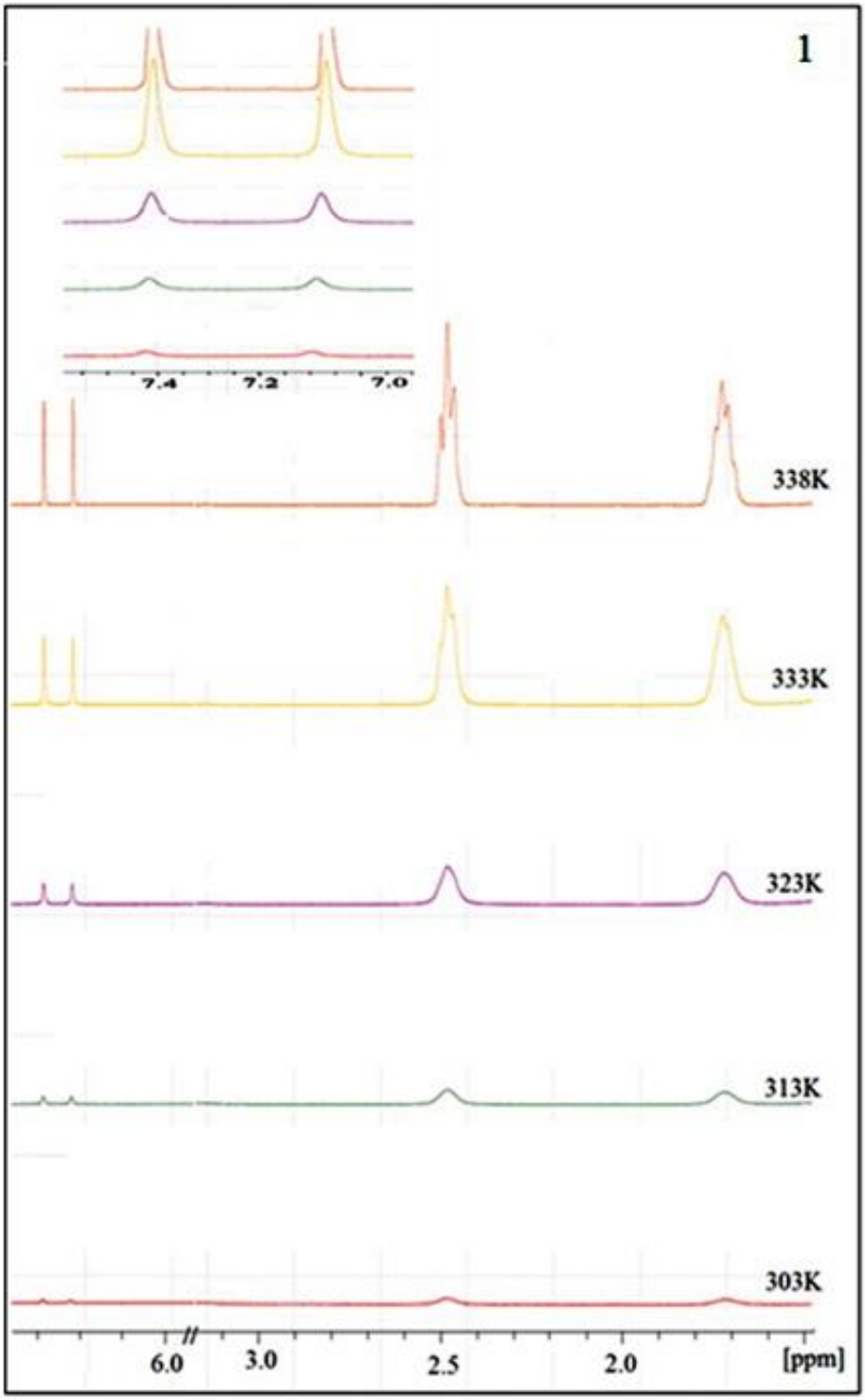

Figure 4.5 Variable temperatures ^{1}HNMR of **1** in CD_3OD. Inset shows the expanded view of aromatic proton of thiazole moiety.

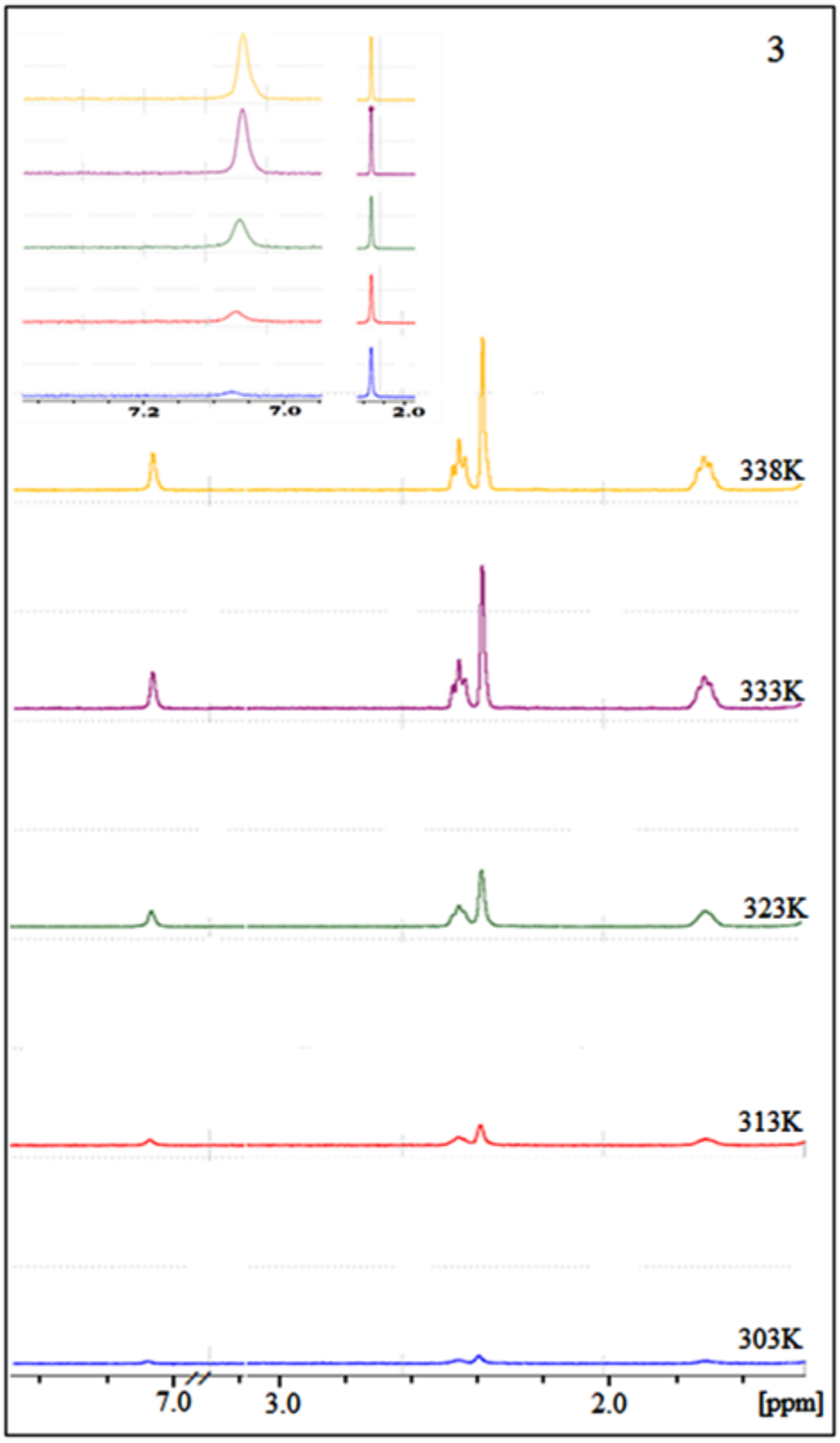

Figure 4.6 Variable temperature ^{1}HNMR of compound **3.** Inset shows the expanded view of aromatic and –CH_3 proton of thiazole moiety.

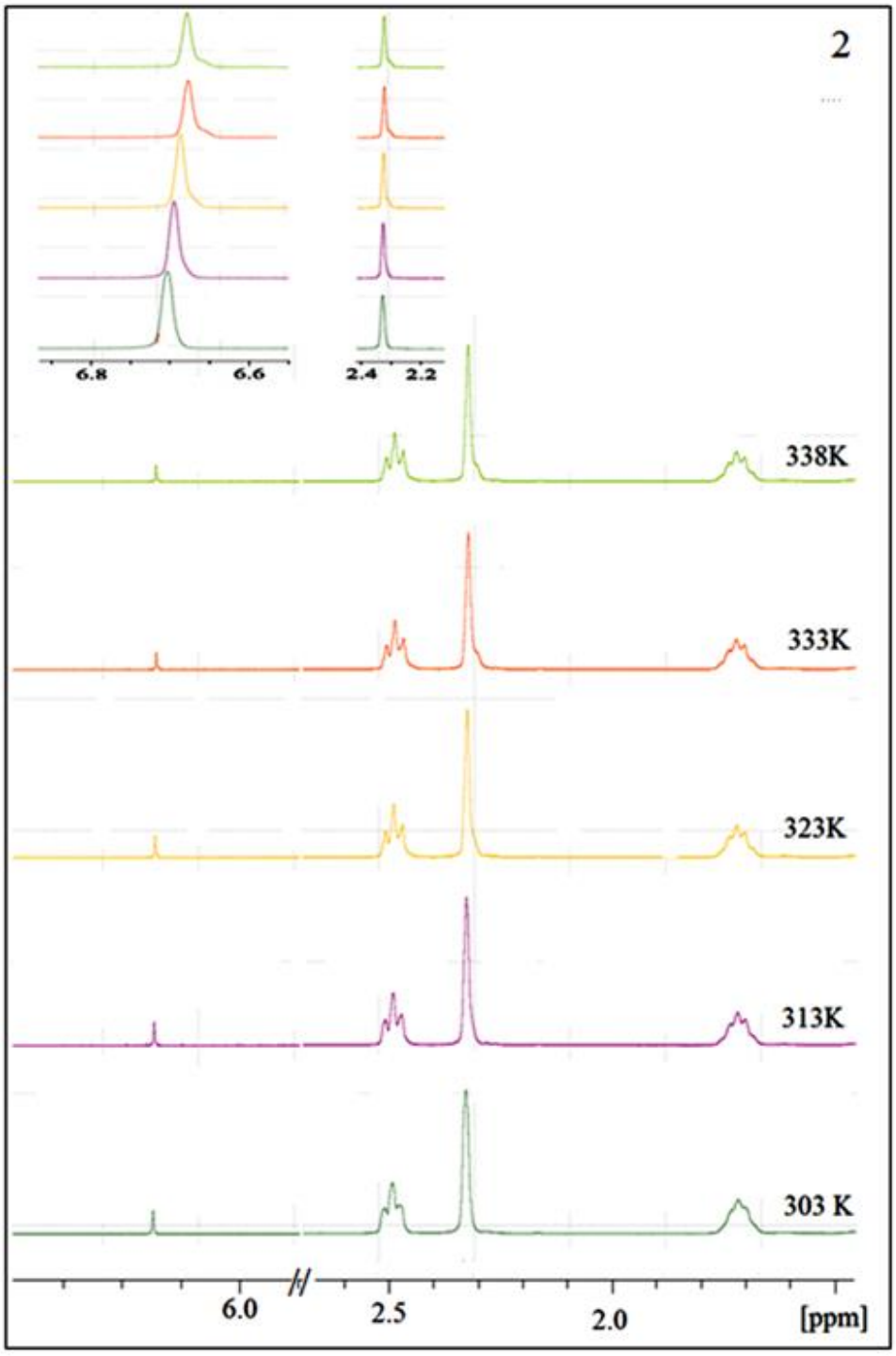

Figure 4.7 Variable temperatures ^{1}HNMR of compound **2.** Inset shows the expanded view of aromatic and –CH_3 proton of thiazole moiety.

H-bonding pattern in all crystal seems to be governed by cyclic (amide) N-H...N (thiazole) synthons[7] along with the intramolecular bond between carbonyl oxygen and thiazole sulphur atom, leading to zero-dimensional (0-D) hydrogen bonded network. A critical examination of the crystal structures demonstrated a weaker hydrogen bond (methyl) C-H....N (thiazole (distance between C...N = 3.496Å, ∟ C-...N = 152.29° for **3**) leading to one-dimensional (1-D) hydrogen bonded network **(Figure 4.8 C)**. Whereas non-gelator **1** showed a robust cyclic (amide) N-H...N (thiazole) supramolecular synthon leading to 0-D hydrogen bonded network along with O...S intramolecular interaction **(Figure 4.8A)**. Understandably, the non-gelling behaviour of gels **1** can be attributed to the absence of one-dimensional hydrogen bonded network which presumably leads to fibre formation and, ultimately to immobilization of solvent.

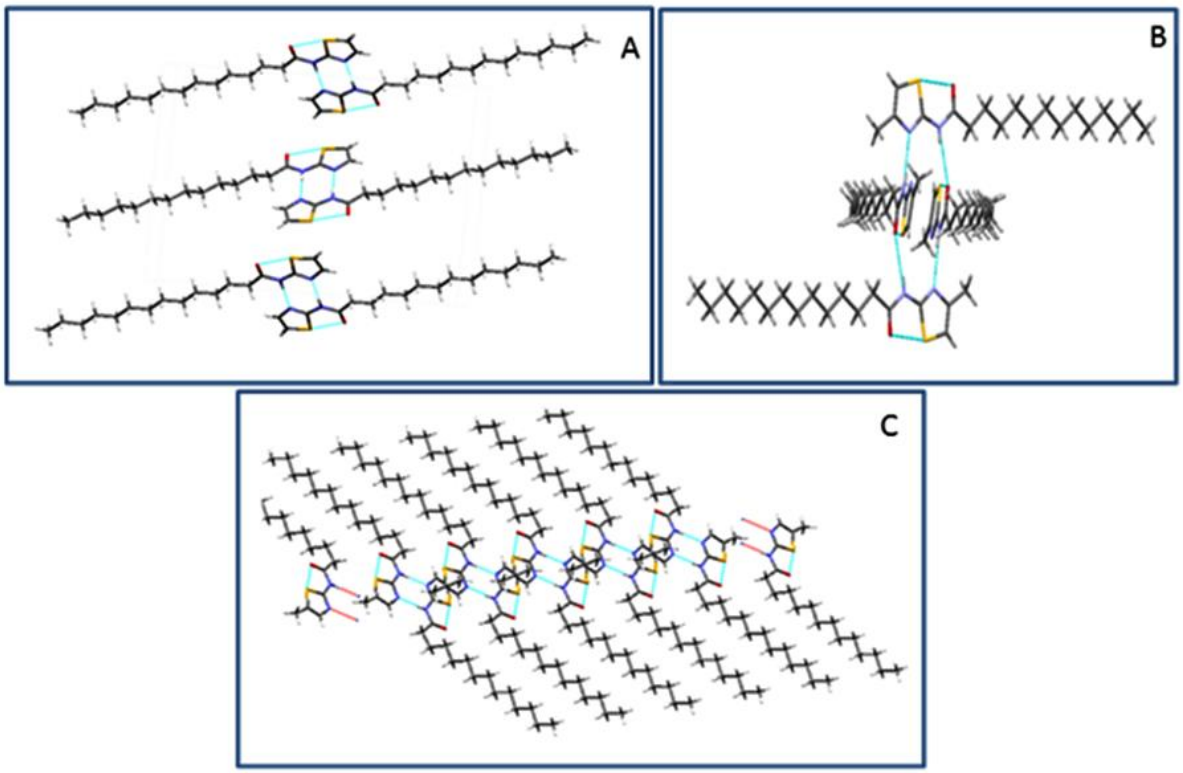

Figure 4.8 Hydrogen bonded network of A) **1,** B) **2** and C) **3.**

Single crystal suitable for non-gelator **2** provided an opportunity to understand the probable reason of its non-gelation behaviour towards all the solvents employed in the present study. A suitable crystal of **2** was obtained from methanol-water (80: 20 v/v) by the slow evaporation method. **2** crystallize out in the monoclinic space group $P2_1/c$ containing two molecules in the asymmetric unit. Four molecules of **2** were found to self- assembled together to form the zero dimensional hydrogen bonded network driven by N-H....N [N...N = 2.884 Å, ∟N-H...N = 173.84°] and N-H...O interaction [N...O = 2.937 Å, ∟N-H...O = 167.09°] (**Figure 4.8B**). A detailed analysis of packing pattern of **2** showed weak van der Waals as the additional force responsible for the overall supramolecules assembly leading to three-dimensional network. We ascertain the presence of a 0-D network, the absence of alkyl chain interdigitation and no additional hydrogen bond such as C-H...N or C-H...O, endowed this molecule incapability to immobilize any solvents.

Understandably, the capability of methyl protons to participate in H-bond depends upon its proximity to electronegative atoms such as N or S[18] as well as on the neighbouring molecule accessibility. In the present class of gelling system, the substitution of a methyl group on the thiazole ring at position 5 or 4 seems to govern the polarity of C-H bonds and ultimately, the strength of the weak H-bond interactions such as C-H...N or C-H...S. It is surprising to see the methyl functionality can induce the gelation as well as proved to be a deterrent to gelation of various solvent depend on its position on thiazole moiety. The proximity of methyl group to an electronegative atom such as N increases its hydrogen bonding capability and leads to more stable 1-D network required for organogelation. Whereas, the presence of methyl group at 4^{th} position on thiazole moiety increase the hydrogen bonding capability of S atom, which is already non- covalently bonded to carbonyl oxygen. So, inductive effect and steric hindrance appear as a guiding force for gelation of polar and non-polar solvents in this class of gelators **(Figure 4.8)**. A weaker H-bond such as C-H...N, C-H...O interactions are considered important as a tool for supramolecular assembly in biological systems,[19] but to the best of our knowledge there is no report on organogelation driven by weaker H-bond such as C-H....N as a driving force for supramolecular gelation.

Table 4.2 Crystallographic parameters of compounds 1, 2 and 3

Crystal data	1	2	3
Empirical formula	$C_{17}H_{30}N_2OS$	$C_{18}H_{32}N_2OS$	$C_{18}H_{32}N_2OS$
Formula weight	310.50	324.53	324.53
Crystal size (mm)	0.18x 0.12 x 0.02	1.0 x 0.8 x 0.56	0.14x 0.11 x 0.03
Crystal system	Monoclinic	Monoclinic	Monoclinic
Space group	P 21/c	P 2_1/c	P 2_1/c
a/Å	23.237(2)	22.1166(3)	22.304(5)
b/Å	4.9497(3)	19.4545(2)	14.610(3)
c/Å	15.6429(12)	9.42062(13)	5.5379(13)
α/°	90	90	90
β/°	90.966(8)	101.1861(13)	91.678(4)
γ/°	90	90	90
Volume/ $Å^{-3}$	1798.93	3976.39(9)	1803.7(7)
Z	1	8	4
D_{calc}	1.5434	1.0841	1.195
F(000)	683.0182	1430.18	712.00
μ (mm^{-1})	1.594	1.461	0.184
Temperature (K)	298	298	293(2)
Observed reflection [$I>2\sigma(I)$]	3383	6244	3541
Parameters refined	190	432	205
Goodness of fit	1.2361	1.3229	1.261
Final R_1 on observed data	0.1181	0.0508	0.0837
Final wR_2 on observed data	0.3352	0.1802	0.1484
Source	Cu K_α	Cu K_α	Mo K_α
Wavelength (Å)	1.5418	1.5418	0.71073
CCDC No.	966725	957407	895760

In order to get an insight into packing of gelator molecules in gel state or the xerogel (dried gel state), powder X-ray diffraction (PXRD) patterns of solid, simulated and xerogel of **3** were compared **(Figure 4.9)** according to the method developed by Weiss et al.[20]

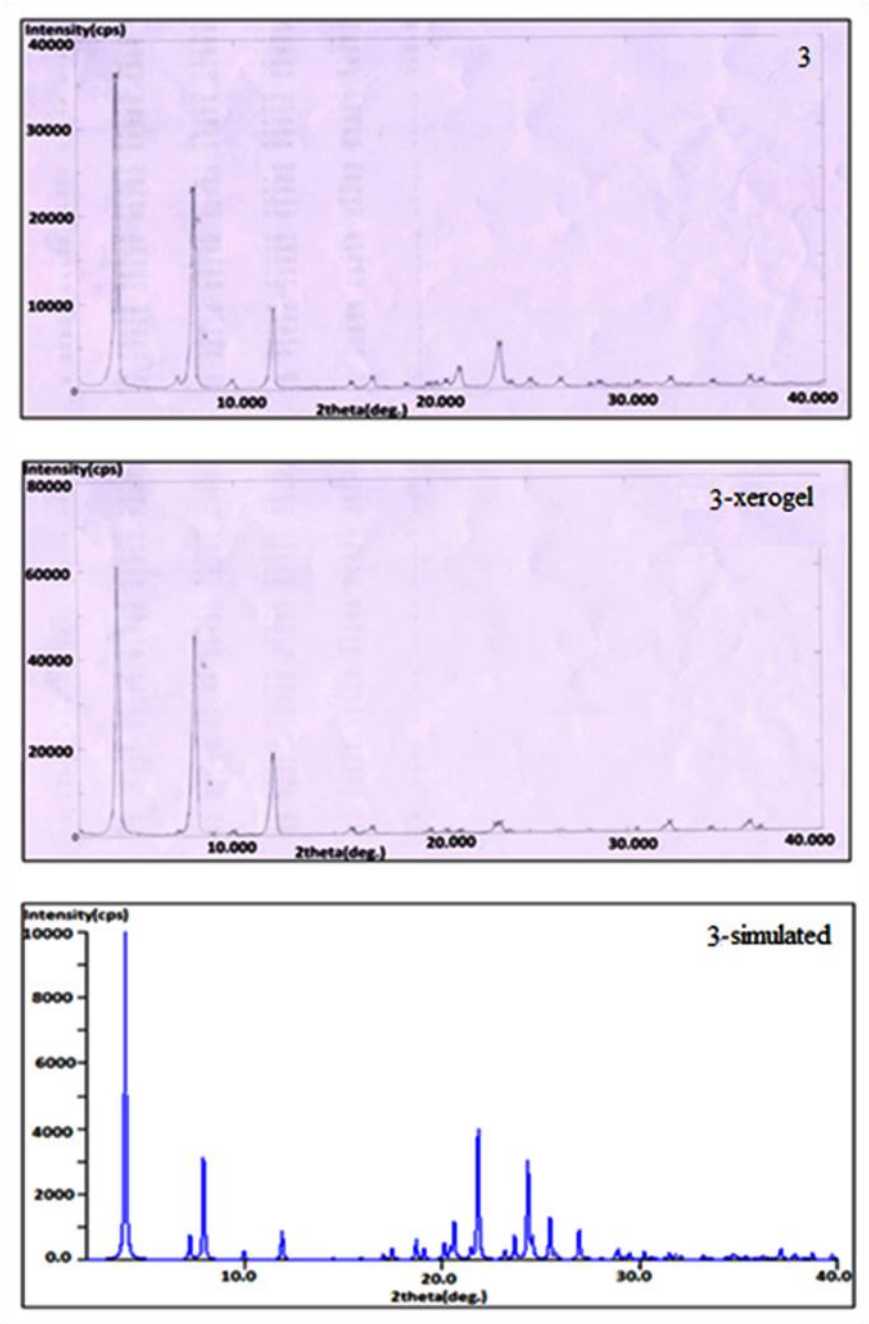

Figure 4.9 comparative powder X-ray diffraction patterns of compound **3** in solid, xerogel and simulated (single crystal structure).

All powder patterns turned out quite similar in all the three states suggesting the retention of hydrogen bonding pattern, which is present in the crystal structure of **3.** The PXRD of **3** showed a periodical high intensity peak position in the lower 2theta angle in the ratio 1:1/2: 1/3 suggesting lamellar packing[9] such as 19.9300, 10.0062, 6.6766 for **3**. Based on various physico-chemical analyses, we propose a plausible mechanism of gelation of **1** and **3** and non-gelation of **2** in **Figure 4.10**.

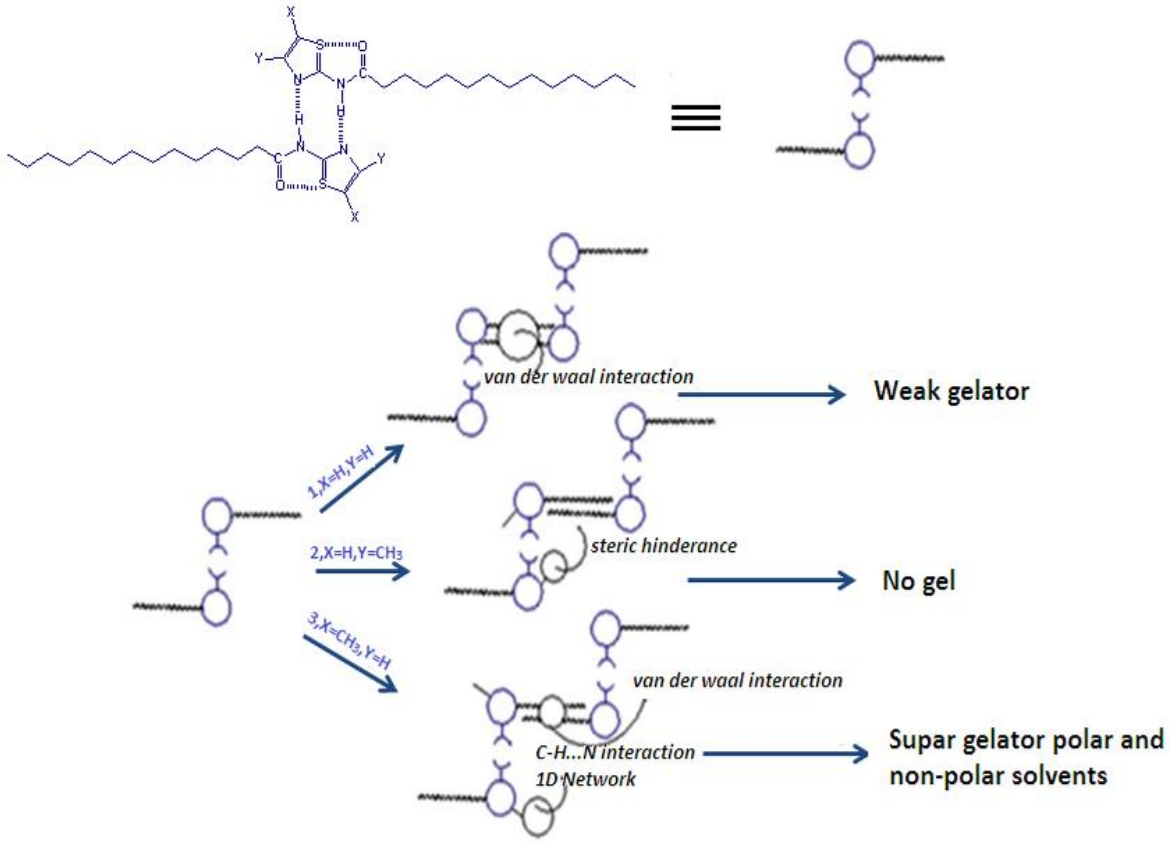

Figure 4.10 Schematic representation of plausible mechanism of gelation (1 and 3) and non-gelation (2).

As evident from crystal structure of **1,** 0-D hydrogen bonded network is extending to 1D through alkyl-alkyl chain interaction suggested the immobilization of non-polar solvent through hydrophobic-hydrophobic interaction after attaining sufficient carbon chain length i.e. 2-tridecanamidothiazole. Gelator **3** showed a combined effect of van der Waals and weak C-H...N interaction as guiding force for supramolecular gelation. The position of methyl group at position 4 in non-gelator **2** appears to disturb the overall supramolecular assembly through steric hindrance leading to 0-D network with less alkyl –alkyl chain interdigitation.

4.4 Conclusions

In conclusion, we have demonstrated a synergistic effect of weak intermolecular forces such as C-H...N and alkyl-alkyl chain interaction as driving force for gelation in amide based thiazole derivatives. Inductive effect and steric effect of a methyl group at various positions in thiazole ring and its proximity to electronegative atoms (N or S) in the heterocyclic rings, seems to govern the hydrogen bonding capability of methyl group leading to 1-D network in **3** and found to be a main guiding force for the enhancement of gelation behaviour of compound **3** over **1**. However, absence of C-H...N interaction and the presence of strong C-H...π or π...π interaction in **2** endowed them with non-gelation property. The suitable substitution of a functional group and exploiting its inducting property in encouraging gelation or non-gelation property may lead to a new strategy to design supramolecular gelling agent. The present study represents first example where the SAFIN of gelling solvents governed by unusual C-H...N interaction, is undoubtedly established in solid, xerogel and gel state with the help of various physico-chemical techniques.

4.5 References

(1)P. Terech ,R.G.Weiss, *Chem. Rev.*, **1997**, 97, 3133.

(2)L.A.Estroff,A.D. Hamilton, *Chem. Rev.*, **2004**, 104, 1201.

(3)J. H. van Esch,B. L. Feringa, *Angew. Chem. Int. Ed.*, **2000**, 39, 2263.

(4)N. M. Sangeetha,U. Maitra, *Chem. Soc. Rev.*, 2005, **34**, 821.

(5)J. W. Steed, *Chem. Soc. Rev.*, **2010**, 39, 3686.

(6)L. E. Buerkle,S. J. Rowan, *Chem. Soc. Rev.*, **2012**, 41**,** 6089.

(7)G. R. Desiraju, *Angew. Chem. Int. Ed.*, **1995**, 34, 2311.

(8)P. Dastidar, *Chem. Soc. Rev.*, **2008**, 37, 2699.

(9)M. George, R. G. Weiss, *Acc. Chem. Res.*, **2005**, 39, 489.

(10)B. Roy, A. Saha, A. Esterrani, A. K. Nandi, *Soft Matter*, **2010**, 6, 3337 and reference cited therein.

(11)P. Yadav, A. Ballabh, *Colloids Surf. A: Physicochem. Eng. Aspects*, **2012**, 414, 333.

(12)J. D. Hartgerink, E. Beniash, S. I. Stupp, *Proc. Natl. Acad. Sci.*, **2002**, 99, 5133.

(13)T. Aida, E. W. Meijer, S. I. Stupp, *Science*, **2012**, 335, 813.

(14)Q.V.Dolomanov,L.B. Bourhis,R.J. Gildea,J.A.K. Howard,H. Puschmann, *J.Appl. Cryst*., **2009**, 42, 339.

(15)G.M.Sheldrick, *ActaCryst.*, **2008**, A64,112.

(16)M. George, R. G. Weiss, *Chem. Mater.*, 2003, **15**, 2879.

(17)J. H. Jung, S. Shinkai ,T. Shimizu, *Chem. Eur. J.*, **2002**, 8, 2684.

(18)R. Taylor , O. Kennard, *J. Am. Chem. Soc.*, **1982**, 104, 5063.

(19)M. Brandl, K. Lindauer, M. Meyer, J. Sühnel, *Theor. Chem. Acc.*, **1999**, 101, 103.

(20)E. Ostuni, P. Kamaras, R. G. Weiss, *Angew. Chem. Int. Ed. Eng.*, **1996**, 35, 1324.

Chapter-4(B)

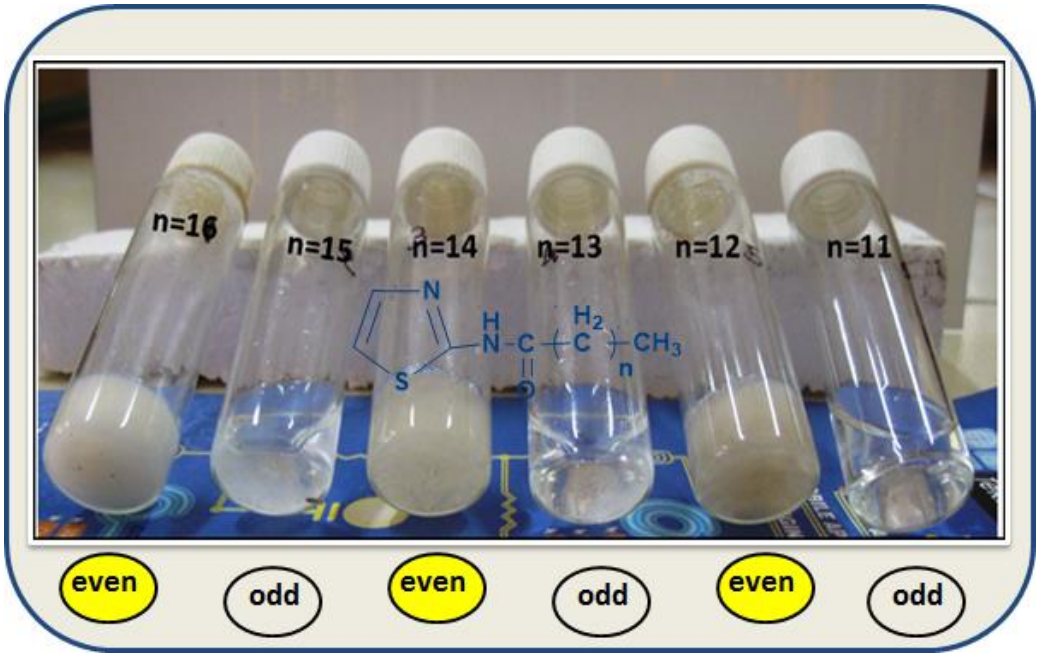

Odd–even effect in a thiazole based organogelator: understanding the interplay of non-covalent interactions on property and applications

Published in New J. Chem., 2015, 39,721-730

4.6 Introduction

Gelling molecules [1-2] self-assemble into various recognizable shapes such as fibers, strands, tapes, ribbons, tubes guided by various non-covalent interactions, which further aggregate to form a three-dimensional (3D) network that immobilizes the solvent molecules. Well defined supramolecular assemblies of gelator fibers throw an opportunity to design and synthesize one-dimensional inorganic nanomaterials, which is otherwise difficult to synthesize by various physical and chemical methods. Therefore, one of the most explored applications of LMOGs is a template directed synthesis of inorganic nanomaterials of various shapes and sizes.[3-8] Numerous gelling systems such as cholesterol based compounds, crown ether appended cholesterol compounds, diamines/sugar based compounds, are well known as structure-directing agent for charged silica and titanium compounds.[9-10] It is well-accepted that gelators having charge or many H-bonding sites would be successful in transcription of silica/titanium compounds(charged precursor) into various shapes and sizes. To the best of our knowledge no such hypothesis/ working rule is available to transcript neutral metal or metal oxide successfully on gelator fibers. Most of the known sol-gel transcriptions of various noble metal or metal oxides are driven by hit and trial method. Therefore, it is required to explore various structural attribute, functional groups, critical balance of hydrophobicity /hydrophilicity required for designed template-directed synthesis of nanomaterial of various shapes and sizes. Moreover, tuning nanomaterial shape and size by systematic variation in gelator structure is also desirable.

We have discussed a new class of LMOGs based on thiazole amide derivatives in former part of this chapter. Interestingly, suitable position of methyl group on thiazole ring, namely, *N*-(5-methylthiazol-2-yl)tetradecanamide (**3**) endowed the gelation property whereas, *N*-(4-methylthiazol-2-yl)tetradecanamide (**2**) completely retard immobilization of solvent. Moreover, thiazole amide derivatives without methyl substitution showed gelation property with lesser extent in terms of less number of solvent gelled and higher minimum gelator concentration (mgc). We proposed the crucial role of a methyl group in participation of weak hydrogen bond formation namely, (methyl)C-H...N, leading to one dimensional hydrogen bonded network, known to be a pre-requisite for organogelation,[11-12] based on single crystal X-ray study of gelator /non-gelator molecules and variable temperature ^{1}HNMR. Moreover,

some of the fundamental questions remained to be answered such as i) is it possible to induce gelation property to a non-gelator by systematic increase in the hydrocarbon chain/hydrophobicity; ii) what is the effect of alkyl chain on gelation behaviour of the molecules in polar solvent or non-polar solvents in this series of compounds? ; iii) is the proposed weak hydrogen bond such as (methyl) C-H...N, robust enough to induce gelation or non-gelation property to a molecule; vi) does the odd-even effect commonly observed in various series of supramolecular gels[13-14] play a role in these series of molecules?; v) how predictable is Supramolecular synthons of amide in the presence of competitive cyclic N-H...N interaction in thiazole based amides? **(Figure 4.11)**; vi) is it possible gain a control over the shape and size of nano-materials synthesized by sol-gel method by a methodical change in the alkyl chain length of gelator molecules?

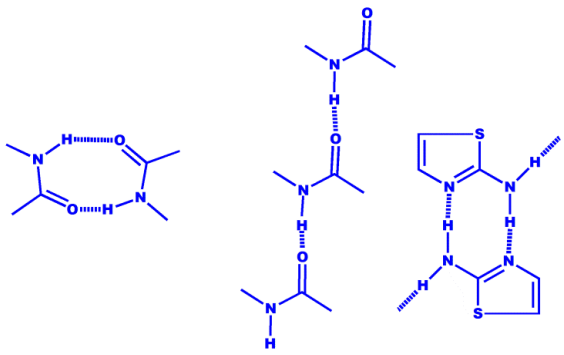

Figure 4.11 Probable Supramolecular synthons in amide and 2-aminothiazole moiety.

In the present study, we decided to systematically increase the alkyl chain length of gelling and non-gelling molecules having methylene group (-CH_2) ranging from (8, 10-16) to understand the interplay of weak hydrogen bond (methyl)C-H...N or (thiazole)C-H...N, C-H...π, etc. along with van der Waals interaction in inducing gelation/non-gelation behaviour **(Figure 4.12)**. The efforts were directed to grow more crystals of gelling/non-gelling molecules in the series. Fortunately, we could grow suitable single crystal of 1b and 3b (n=10, even) along with 1c and 3c (n=9, odd), which helped us in understanding the cause of even/odd effect on gelation behaviour.

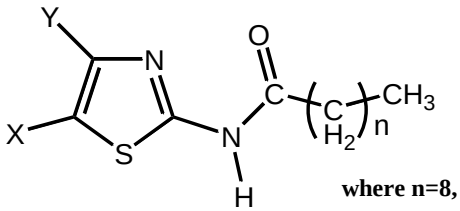

where n=8, 10,11,12,13,14,15,16

If X= H, Y= H, 1a-1h
X= H, Y= CH_3, 2a-2h
X= CH_3, Y= H, 3a-3h

Figure 4.12 List of compounds synthesized.

The potential application of gelators (**3a-3h**) as a template for synthesis of silver and zinc oxide (ZnO) nanomaterial were explored. Template direct synthesis of ZnO nanoparticles was undertaken due to its intriguing chemical, electrical, mechanical and optical properties along with potential application in solar cells, hydrogen-storage, gas sensors, liquid crystal displays, etc.[15-17] Moreover, the properties and applications of the ZnO nanoparticles strongly dependents upon their structures and morphologies.

4.7 Experimental Section

4.7.1 Materials and physical measurements

2-aminothiazole (97%), 2-amino-5-methylthiazole (98%), 2-amino-4-methylthiazole (98%), Octadecanoic acid (97%), Heptadecanoic acid (>98%), Hexadecanoic acid (98%), Pentadecanoic acid (99%), Tridecanoic acid(97%), Dodecanoic acid (98%), Decanoic acid(96%) (All from Aldrich) were used as received. The other chemicals were of the highest commercial grade available and were used without further purification. The solvents used for the preparation of gels were reagent grade. All solvents used in the synthesis were purified, dried and distilled as required.

All thiazole based amide derivatives were synthesized by reacting the acid chloride of various aliphatic acids with thiazole derivatives using a modified synthetic procedure.[18] A detailed synthesis, characterization and gelation properties of compounds **1d**, **2d** and **3d** is already discussed as compound 1,2 and 3 respectively in previous part of this chapter. All new compounds synthesized in the present study were characterized by IR, ^{1}H-NMR, and MS analysis.

FT-IR spectra were recorded on a Perkin Elmer –RX FT-IR instrument. Solid samples were recorded as an intimate mixture with powdered KBr. The ^{1}H- NMR spectra were measured by using a Bruker AVANCE, 400MH_Z with TMS as internal standard.

Morphologies of all reported xerogel (dried gel) were investigated by using scanning electron microscopy (SEM) (JEOL JSM5610 LV microscope). For SEM study, the hot sample (gel liquid) was placed over the SEM sample holder and allowed to form the gel. Then, the sample was subjected to dryness under normal room temperature and pressure and coated with carbon (**1e**, **1h**, **and 3e-3g**) or gold sputtering (**3h**). The morphologies of synthesized Ag and ZnO nanoparticles were investigated using transmission electron microscope (TEM) (Philips CM 200) in the working voltage of 20-200kV. TEM studies were carried out by placing a small amount of the corresponding compound dispersed in ethanol/water on carbon-coated copper grids and dried by slow evaporation. Powder diffraction patterns of neat xerogel **1e** (methanol, slowly evaporated) and xerogel loaded with silver nanoparticles was recorded on XPERT Philips (CuKα radiation). The silver nano-particles loaded on gelator fibres was subjected to powder diffraction studies using Bruker D8 (CuKα radiation) diffractometer. Single crystal X-ray study of compounds **2d** and **3c** was carried out on Single Crystal X-ray diffractometer (Xcalibur, EOS, Gemini diffractometer) at 298 K. The structure was solved using olex2[19] structure solution programme using charge flipping and refined with olex2.refine[20] refinement package using Gauss-Newton minimization.

4.7.2 General Synthesis methodology

Oxalyl chloride (2ml, 20 mmol) was added slowly to a stirred solution of Monocarboxylic acids (2 mmol) in dry dichloromethane (10mL) under a nitrogen atmosphere. The mixture was stirred under a nitrogen atmosphere for 12 h. Excess oxalyl chloride and solvent were removed by distillation under reduced pressure. The acid chloride obtained was dissolved in dry dichloromethane (10 mL) and added to the aminothiazole (2 mmol) in triethylamine (0.3ml, 2.15mmol). The mixture was stirred overnight under a nitrogen atmosphere .The reaction mixture was then added to dilute hydrochloric acid (5%), and extracted with chloroform. The product residue after removing chloroform was purified by repeated crystallization from ethyl acetate/pet. ether mixture.

4.7.3 Gelation Test

A weighted amount of potential gelator (1wt %) and a measured volume of selected pure solvent were placed into a test tube and the system was heated in an oil or water bath until all solid materials got dissolved. The solution was cooled to ambient temperature and finally, the test tube was turned upside down to observe if the solution inside could still flow. A positive test is obtained if the flow test is negative. Gel-to-sol transition temperatures (T_{gel}) were determined by using a conventional "falling ball" method. In this test, a small glass ball (63mg) was carefully placed on the top of the gel to be tested, which was produced in a test tube. The tube was slowly heated in a thermostated oil bath until the ball fell to the bottom of the test tube. The temperature at which the ball reaches at the bottom of the test tube is taken as T_{gel} of that system.

4.7.4 Synthesis of Silver nanoparticle.

In order to load the organogels with $AgNO_3$ for the synthesis of silver nanostructure, $AgNO_3$ (2 mg) and the gelator (2 wt %) was dissolved in ethanol (2ml) by heating. The solution was allowed to stand to form colourless gel. The gel was irradiated with a mercury vapour UV lamp. On irradiation, there was visually observable change to the gel, the colour rapidly changed from colourless to pale pink within 15 minutes of irradiation and it changes to reddish brown over a period of an hour.

4.7.5 Synthesis of ZnO nanoparticle.

In order to prepare ZnO particles, 35 mg zinc acetate was mixed with 10 mg KOH in 1 ml ethanol. This was added to a solution containing 20 mg gelator in 1.0 ml ethanol. This mixture was heated and finally allowed to cool.A white gel was obtained which was allowed to stand for a day at ambient temperature and then dried in a vacuum. In order to remove the Template, the sample was then heated to 400°C for 4 hr.[21]

4.7.6 Antibecterial Activity.

The compounds were tested in-vitro for their antibacterial activity against two microorganisms viz. E.coli and S.aureus which are pathogenic in human beings.1000 μg cm^{-3} compound 1f (C) and 100μg cm^{-3}silver nanoparticles loaded inside gel matrix (N) are suspended in DMSO by sonication. The colony of *E. coli* and S.aurus

were cultured on LB agar plates and 10 µl of the prepared solution was supplemented to examine the bactericidal effect of silver nanoparticles.

4.7.7 Analytical data

N-(thiazol-2-yl)decanamide (**1a**): Yield 78%, m.p. 105 °C,^{1}H NMR (400MH$_Z$, $CDCl_3$, TMS); δ12.013(s,1H;NH),7.458 (d, 1H; CH), 7.024 (d,1H;CH), 2.581-2.544(t,2 H;CH_2), 1.828-1.753 (m,2H,CH_2),1.407-1.266 (m,12H,CH_2), 0.912-0.878 (t,3H;CH_3). MS (EI): m/z 254.23$[M]^+$. FT-IR(KBr): 3456, 3172, 2848, 1690, 1576, 1495, 1467, 1424, 1378, 1325, 1274, 1213, 1175, 1068, 960, 873, 810, 777, 625, 519, 474 cm^{-1}.

N-(thiazol-2-yl)dodecanamide **(1b)**: Yield 82%, m.p. 116°C, ^{1}H NMR (400MH$_Z$, $CDCl_3$, TMS); δ 12.291(s,1H;NH),7.458 (d,1H;CH), 7.029 (d,1H;CH), 2.595-2.557 (t,2H;CH_2),1.830-1.754 (m,2H, CH_2), 1.425-1.266 (m,16H,CH_2), 0.908-0.874 (t,3H;CH_3). MS (EI): m/z 281.85$[M]^+$. FT-IR(KBr): 3450, 3271, 3180, 2916, 2849, 1687, 1580, 1467, 1422, 1381, 1327, 1278, 1204, 1115, 1065, 960, 810, 776, 625, 519, 417 cm^{-1}.

N-(thiazol-2-yl)tridecanamide **(1c)**: Yield 76%, m.p.110 °C, ^{1}H NMR (400MH$_Z$, $CDCl_3$, TMS); δ 12.162(s,1H;NH),7.458 (d, 1H; CH), 7.282 (d, 1H;CH), 2.587-2.549 (t,2H;CH_2),1.827-1.752 (m,2H, CH_2), 1.424-1.265 (m, 18H, CH_2), 0.909-0.875 (t, 3H; CH_3). MS (EI): m/z 295.81$[M]^+$. FT-IR(KBr): 3484, 3176, 2944, 1691, 1560, 1492, 1468, 1319, 1274, 1175, 1063, 960, 874, 777, 714, 626, 520 cm^{-1}.

N-(thiazol-2-yl)pentadecanamide **(1e):** Yield 85%, m.p. 105°C, ^{1}H NMR (400 MHz, $CDCl_3$, TMS): δ12.165(s,1H;NH),7.457 (d, 1H; CH), 7.023(d, 1H; CH), 2.590-2.553 (t, 2H; CH_2), 1.827-1.752(m, 2H, CH_2), 1.424-1.264 (m, 22H, CH_2), 0.910-0.876(t, 3H;CH_3). MS (EI): m/z 324.11 $[M]^+$. FT-IR (KBr): 3171, 2916, 2849, 1688, 1577, 1468, 1321, 1279, 1166, 1065, 959, 874, 805, 778, 624, 520 cm^{-1}.

N-(thiazol-2-yl)hexadecanamide **(1f):** Yield 80%, m.p 121 °C, ^{1}H NMR (400 MHz, $CDCl_3$, TMS): δ7.458 (d, 1H; CH), 7.026(d, 1H; CH), 2.585-2.547(t, 2H; CH_2), 1.888-1.771(m, 2H, CH_2), 1.424-1.265 (m, 24H, CH_2), 0.911-0.876(t, 3H; CH_3). MS (EI): m/z 338.31$[M]^+$. FT-IR(KBr): 3174, 2917, 2849, 1686, 1581, 1468, 1380, 1322, 1288, 1110,1067, 959, 873, 777, 718, 625, 520 cm^{-1}.

N-(thiazol-2-yl)heptadecanamide **(1g):** Yield 83%, m.p. 117 °C, ^{1}H NMR (400 MHz $CDCl_3$, TMS): δ11.985(s,1H;NH),7.462 (d, 1H; CH), 7.032(d, 1H; CH), 2.590-2.365(t, 2H; CH_2), 1.827-1.752(m, 2H, CH_2), 1.437-1.264(m, 26H, CH_2), 0.911-0.877(t, 3H; CH_3). MS (EI): m/z 352.74$[M]^+$. FT-IR (KBr): 3170, 2917, 2849, 1685, 1576, 1469, 1379, 1321, 1272, 1168, 1064, 959, 875, 778, 718, 624, 520 cm^{-1}.

N-(thiazol-2-yl)octadecanamide **(1h):** Yield 79%, m.p. 102 °C, ^{1}H-NMR (400 MHz, $CDCl_3$, TMS): δ11.983(s,1H;NH),7.457 (d, 1H; CH), 7.020(d, 1H; CH), 2.581-2.544(t, 2H; CH_2), 1.828-1.753(m, 2H, CH_2), 1.430-1.265 (m, 28H, CH_2), 0.914-0.877(t, 3H; CH_3). MS (EI): m/z 366.14 $[M]^+$. FT-IR (KBr): 3176, 2924, 2851, 1683, 1580, 1465, 1379, 1323, 1275, 1169, 1065, 962, 872, 774, 718, 623, 520 cm^{-1}.

N-(4-methylthiazol-2-yl)decanamide **(2a):** Yield 69%, m.p. 64°C, ^{1}H NMR(400MH_Z, $CDCl_3$, TMS) : δ 6.564 (s,1H;CH), 2.611-2.573 (t,2H,CH_2), 2.407 (s,3H;CH_3),1.767-1.730 (m,2H; CH_2), 1.328-1.261 (m,12H;CH_2) 0.891-0.879 (t,3H;CH_3). MS (EI): m/z 267.86 $[M]^+$. FT-IR (KBr): 3481, 2857, 1882, 1697, 1567, 1567, 1465, 1377, 1319, 1280, 1213, 1115, 1080, 1017, 956, 846, 723, 644, 602, 525, 473 cm^{-1}.

N-(4-methylthiazol-2-yl)dodecanamide **(2b):** Yield 70%, m.p. 90 °C. ^{1}HNMR (400 MH_Z, $CDCl_3$,TMS):δ13.364(s,1H;NH),6.564 (s,1H;CH), 2.611-2.573 (t,2H,CH_2) , 2.407 (s,3H; CH_3), 1.767-1.730 (m,2H;CH_2), 1.328-1.261 (m,16H;CH_2), 0.891-0.879 (t,3H;CH_3). MS (EI): m/z 296.67$[M]^+$. FT-IR(KBr): 3540, 3170, 2850, 1904, 1695, 1562, 1465, 1278, 1167, 1072, 956, 848, 645, 572, 538, 475, 425 cm^{-1}.

N-(4-methylthiazol-2-yl)tridecanamide **(2c):** Yield 76%, m.p 71 °C,^{1}H NMR (400MH_Z ,$CDCl_3$,TMS):δ13.350(s,1H;NH),6.649 (s,1H;CH), 2.702-2.664 (t,2H,CH_2), 2.515 (s,3H; CH_3), 1.805-1.769 (m,2H;CH_2), 1.314-1.221 (m,18H;CH_2), 0.911-0.877 (t,3H;CH_3). MS (EI): m/z 310.48$[M]^+$. FT-IR(KBr): 3536, 3175, 2915, 1905, 1694, 1567, 1552, 1467, 1276, 1167, 1130, 1075, 1001, 949, 846, 774, 721, 641, 573, 533, 409 cm^{-1}.

N-(4-methylthiazol-2-yl)pentadecanamide **(2e)**: Yield 72%, m.p.100 °C, ^{1}H NMR (400 MHz, $CDCl_3$, TMS): δ6.529 (s, 1H; CH), 2.561-2.523(t,2H;CH_2), 2.371 (s,3H; CH_3), 1.769-1.666 (m,2H;CH_2), 1.330-1.262 (m,22H;CH_2), 0.911-0.880(t,3H;CH_3). MS (EI): *m/z* 338.25$[M]^+$. FT-IR (KBr): 3358, 3164, 2928, 2854, 1672, 1553, 1469,

1314, 1235, 1115, 1079, 974, 772, 564 cm^{-1}.

N-(4-methylthiazol-2-yl)hexadecanamide **(2f)**: Yield 70%, m.p. 100 °C, ^1H NMR (400MHz, $CDCl_3$, TMS); δ13.360(s,1H;NH),6.652(s, 1H; CH) 2.698-2.660 (t,2H; CH_2), 2.511 (s,3H; CH_3),1.801-1.765 (m, 2H;CH_2), 1.377-1.311(m,24H;CH_2), 0.908-0.874 (t,3H;CH_3). MS (EI): *m/z* 351.86$[M]^+$. FT-IR (KBr): 3348, 3152, 2914, 2849, 1670, 1552, 1461, 1317, 1233, 1117, 1085, 976, 778, 561 cm^{-1}.

N-(4-methylthiazol-2-yl)hetadecanamide **(2g):** Yield 74%, m.p.100 °C, ^1H NMR (400 MHz, $CDCl_3$, TMS);δ13.345(s,1H;NH),6.649(s, 1H; CH), 2.702-2.664 (t,2H; CH_2), 2.515 (s,3H; CH_3), 2.385-2.348 (m, 2H; CH_2), 1.316-1.268(m,26H;CH_2), 0.911-0.877 (t,3H; CH_3). MS (EI): *m/z* 366.40$[M]^+$. FT-IR (KBr): 3359, 3160, 2923, 2859, 1675, 1559, 1463, 1329, 1239, 1121, 1090, 982, 770, 569 cm^{-1}.

N-(4-methylthiazol-2-yl)octadecanamide **(2h)**: Yield 71%, m.p.100 °C, ^1H NMR (400 MHz, $CDCl_3$, TMS): δ6.559(s, 1H; CH), 2.501-2.463(t,2H;CH_2), 2.238 (s,3H; CH_3), 1.756-1.720 (m, 2H;CH_2), 1.331-1.267(m,28H;CH_2), 0.912-0.877(t,3H;CH_3). MS (EI): *m/z* 380.07$[M]^+$. FT-IR (KBr): 3355, 3154, 2918, 2851, 1678, 1552, 1468, 1311, 1233, 1111, 1089, 976, 777, 560 cm^{-1}.

N-(5-methylthiazol-2-yl)decanamide **(3a):** Yield 81%, m.p. 102 °C, ^1H NMR (400MH_Z, m/z $CDCl_3$, TMS): δ12.191(s,1H;NH),7.063 (s,1H; CH), 2.539-2.502 (t,2H;CH_2), 2.432 (s,3H;CH_3),1.808-1.733 (m,2H;CH_2), 1.415-1.292 (m,12H;CH_2), 0.905-0.871 (t,3H;CH_3). MS (EI): m/z 268.25 $[M]^+$. FT-IR (KBr): 3448, 3181, 3059, 2918, 1697, 1583, 1461, 1410, 1378, 1311, 1279, 1112, 1071, 922, 874, 672, 527, 496 cm^{-1}.

N-(5-methylthiazol-2-yl)dodecanamide **(3b):** Yield 79%, m.p. 114 °C, ^1H NMR (400MH_Z, $CDCl_3$, TMS); δ 7.135 (s,1H; CH), 2.610 – 2.573 (t,2H;CH_2), 2.457 (s,3H; CH_3), 1.813-1.739 (m,2H;CH_2), 1.388-1.268 (m,16H; CH_2) , 0.910-0.893(t,3H;CH_3). MS (EI): m/z 295.93 $[M]^+$. FT-IR (KBr): 3482, 3180, 3059, 2918, 1698, 1586, 1463, 1410, 1379, 1312, 1280, 1211, 1165, 1112, 1068, 940, 835, 786, 722, 673, 527, 428 cm^{-1}.

N-(5-methylthiazol-2-yl)tridecanamide **(3c):** Yield 83%, m.p. 106°C, ^1H NMR (400MH_Z, $CDCl_3$, TMS): δ 7.063 (s,1H; CH), 2.542-2.504 (t,2H;CH_2), 2.434

(s,3H;CH_3), 1.802-1.732 (m,2H;CH_2), 1.398-1.265 (m,18H;CH_2), 0.912-0.875 (t,3H;CH_3). MS (EI): m/z 310.40$[M]^+$. FT-IR (KBr): 3444, 3267, 3185, 2917, 1681, 1587, 1463, 1418, 1379, 1303, 1164, 1081, 958, 827, 796, 718, 625, 525 cm^{-1}.

N-(5-methylthiazol-2-yl)pentadecanamide **(3e):** Yield 78%, m.p.105 °C, ^1H NMR (400MHz, $CDCl_3$, TMS): δ7.084(s, 1H; CH), 2.538-2.500 (t,2H;CH_2), 2.442 (s,3H; CH_3), 1.788-1.734 (m, 2H;CH_2), 1.278-1.266 (m,22H;CH_2), 0.912-0.878 (t,3H;CH_3). MS (EI): *m*/*z* 338.19$[M]^+$.FT-IR(KBr): 3179, 3060, 2912, 2847, 1682, 1589, 1466, 1418, 1381, 1303, 1279, 1181, 958, 719, 526 cm^{-1}.

N-(5-methylthiazol-2-yl)hexadecanamide **(3f)**: Yield 82%, m.p.121°C, ^1H NMR (400 MHz, $CDCl_3$, TMS): δ 11.997(s,1H;NH),7.061 (S, 1H; CH), 2.534-2.497(t,2H;CH_2), 2.431(s,3H;CH_3), 1.808-1.739 (m, 2H;CH_2), 1.267-1.224 (m,24H;CH_2), 0.912-0.878 (t,3H;CH_3). MS (EI): *m*/*z* 352.20$[M]^+$. FT-IR(KBr): 3427, 3180, 3080, 2919, 2850, 1697, 1585, 1462, 1409, 1381, 1311, 1280, 1111, 953, 832, 723, 527 cm^{-1}.

N-(5-methylthiazol-2-yl)heptadecanamide **(3g)**: Yield 80%, m.p.111 °C, ^1H NMR (400 MHz, $CDCl_3$,TMS): δ11.879(s,1H;NH),7.062(s, 1H; CH) 2.532-2.494(t, 2H; CH_2), 2.431 (s,3H; CH_3), 1.808-1.734 (m, 2H;CH_2), 1.267-1.224(m,26H;CH_2),0.912-0.893(t,3H;CH_3). MS (EI): *m*/*z* 366.24$[M]^+$. FT-IR (KBr): 3432, 3181, 2919, 2850, 2274, 1697, 1588, 1472, 1380, 1312, 1166, 1112, 1067, 962, 831,782, 622 cm^{-1}.

N-(5-methylthiazol-2-yl)octadecanamide **(3h)**: Yield 79%, m.p.108 °C, ^1H NMR (400 MHz, $CDCl_3$, TMS): δ11.899(s,1H;NH),7.088(s, 1H; CH), 2.533 -2.515 (t,2H; CH_2), 2.497 (s,3H; CH_3), 1.787-1.752 (m, 2H;CH_2), 1.331-1.266(m,28H;CH_2), 0.912-0.878(t,3H; CH_3). MS (EI): *m*/*z* 380.05$[M]^+$. FT-IR (KBr): 3428, 3179, 2919, 2850, 1696, 1583, 1465, 1411, 1380, 1311, 1278, 1168, 1108, 793, 722 cm^{-1}

4.8 Results and Discussion

4.8.1Gelation behaviour

In the present study, gelation abilities of **1a-1h, 2a-2h** and **3a-3h** were examined in a variety of polar and apolar solvents **(Table 4.3)** by a systematic increase in the alkyl chain length (n=8-16). As we know that flexible alkyl chain length is an important structural component which can influence organogelation behaviour significantly.[22-23] To understand role of alkyl chain along with additional methyl group a shorter alkyl

chain compound, 5-methyl-2-decanamidothiazole **3a** was synthesized and tested for gelation. Compound **3a** turned out to be a non-gelator suggesting critical aliphatic chain is required to induce gelation. As expected **1a** (2-decanamidothiazole) and **2a** (4-methyl-2-decanamidothiazole) also turned out to be a non-gelator. Hence, we may conclude that the aliphatic carbon chain length of 12 carbons or more was found to be critical for immobilization of solvents in case of, **3a-3h** and 14 carbons or more for **1a-1h.** Unsubstituted (**1a-1h**) and 5-methyl substituted (**3a-3h**) thiazole amides displayed excellent gelation properties towards various solvents such as methanol, ethanol, octadecane, etc. with low minimum gelation concentration (mgc) (wt%, w/v). A significant enhancement and/or retardation of gelation property in the new series of compounds with increase in methylene group, was observed.

Table 4.3 Gelation studies of compounds 1a-1h, 2a-2h and 3a-3h

Solvents	1a	1b	1c	1d	1e	1f	1g	1h
Methanol	S	C	C	G (1.86)	W.G	G (1.46)	C	G (2.60)
Ethanol	S	S	C	G (2.16)	W.G	G (1.49)	C	G (4.06)
n-pentanol	S	S	S	G (2.80)	S	G (2.73)	S	G (7.46)
n-heptanol	S	S	S	S	S	G (3.31)	S	G (9.90)
Water	P	P	P	P	P	P	P	P
THF	S	S	S	S	S	S	S	S
Iso octane	S	P	P	G (2.42)	P	P	P	P
Xylene	S	S	C	C	C	P	C	S
Cyclohexane	P	P	P	G (2.40)	P	P	P	P
n-octadecane	P	W.G	G (1.00)	G (0.70)	G (1.47)	G (0.69)	G (0.901)	G (1.10)

G=gel, P=precipitate, C=crystals, S=solution, values in the parenthesis represent MGC (minimum gelator concentration) in wt %(g/100mL of solvent)

Table 4.3 Continued...

Solvents	2a	2b	2c	2d	2e	2f	2g	2h
Methanol	S	S	S	S	S	S	S	S
Ethanol	S	S	S	S	S	S	S	S
n-pentanol	S	S	S	S	S	S	S	S
n-heptanol	S	S	S	S	S	S	S	S
Water	P	P	P	P	P	P	P	P
THF	S	S	S	S	S	S	S	S
Iso octane	S	S	S	S	P	P	P	P
Xylene	S		S	S	P	P	P	P
Cyclohexane	S	P	S	P	P	P	P	P
n-octadecane	S	P	S	P	S	S	S	S

Solvents	3a	3b	3c	3d	3e	3f	3g	3h
Mthanol	S	G (2.57)	G (2.11)	G (0.65)	G (0.68)	G (0.48)	G (0.73)	G (0.70)
Ethanol	S	G (2.82)	G (2.17)	G (0.80)	G (1.05)	G (0.66)	G (0.88)	G (0.70)
n-pentanol	S	G (4.44)	G (4.20)	G (2.12)	G (2.96)	G (2.33)	G (2.94)	G (0.32)
n-heptanol	S	G (4.76)	G (4.92)	G (3.83)	G (3.14)	G (3.19)	G (4.23)	G (0.39)
Water	P	P	P	P	P	P	P	P
THF	S	S	S	S	S	S	S	S
iso octane	P	P	P	G (0.90)	G (1.50)	G (1.05)	P	P
Xylene	S	S	S	P	P	P	S	S
Cyclohexane	P	P	P	G (3.17)	P	G (2.56)	P	P
n-octadecane	P	G (2.21)	G (2.37)	G (1.16)	G (1.42)	G (1.30)	G (2.29)	G (2.42)

Compounds **1a-1h** displayed an interesting gelation behaviour with the increase in methylene group in alkyl chain, the compounds having an even number of methylene group (n=even) were outstanding organogelators, whereas compounds having an odd number of methylene group were non-gelator. For example, Compounds **1d** (n=12), **1f** (n=14) and **1h** (n=16) demonstrated organogelation and compounds **1c** (n=11), **1e** (n=13) and **1g** (n=15) showed no-gelation at all **(Figure 4.13)**. The effect of the odd-even number of methylene group of alkyl chain on the gelation behaviour of these series of compounds is quite pronounced.

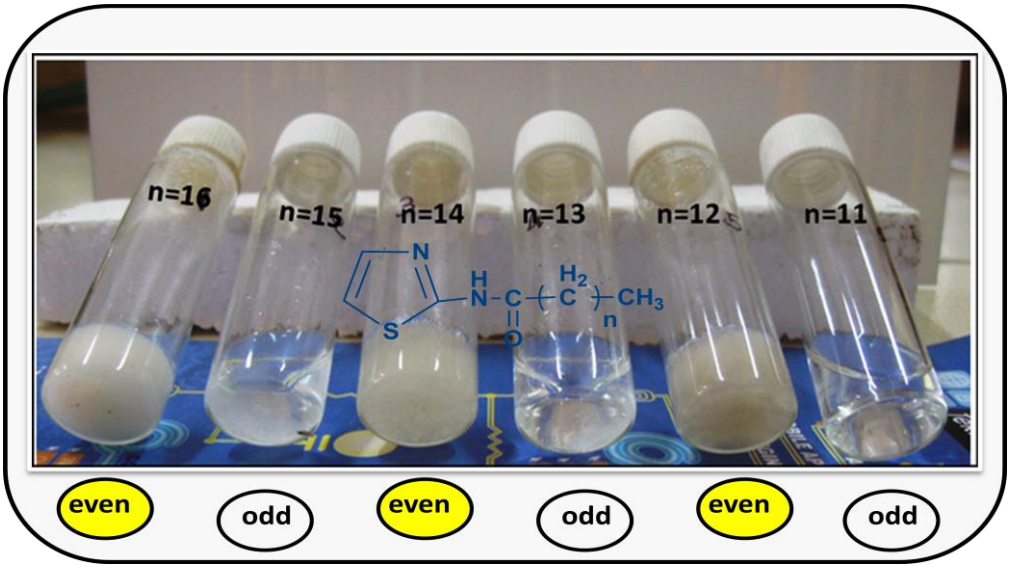

Figure 4.13 Odd-even effect of compounds 1c-1h in methanol (n=number of methylene group in alkyl chain).

Similarly, the series of gelators (**3b-3h**) with odd number of methylene units (n= 11, 13, 15) in the alkyl tail required large amount of gelling compound to exhibit immobilization of solvent (larger mgc value) as compare with compounds having even number of methylene units (n=10,12,14,16) suggested the role of odd-even effect on gelation behaviour. Moreover, the odd-even effect of methylene group of alkyl chain becomes more effective after reaching a critical chain length, i.e. n >12 in the series of thiazole amides. A representative graph to show the effect of increase in number of methylene group 'n' in the aliphatic chain length of thiazole amides (**3b-3h**) to critical gelator concentration (mgc) (wt % , w/v) in methanol is shown in **Figure 4.14**.

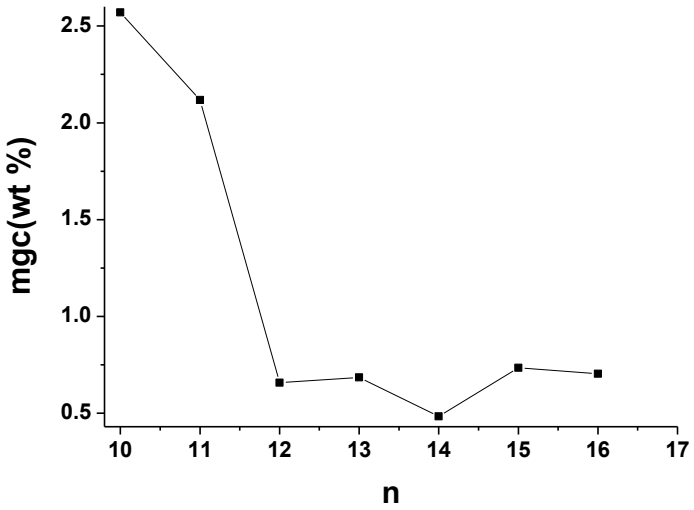

Figure 4.14 minimum gelator concentration (wt %, w/v) of 3b-3h in methanol versus number of methylene groups (n).

Concentration-dependent gelation studies of all the gelators were carried out in ethanol. The dependence of T_{gel} on the concentration of gelator in ethanol is shown in **Figure 4.15**. T_{gel} increases rapidly with concentration upto certain wt % and then showed independence towards the increase in concentration of gelator.

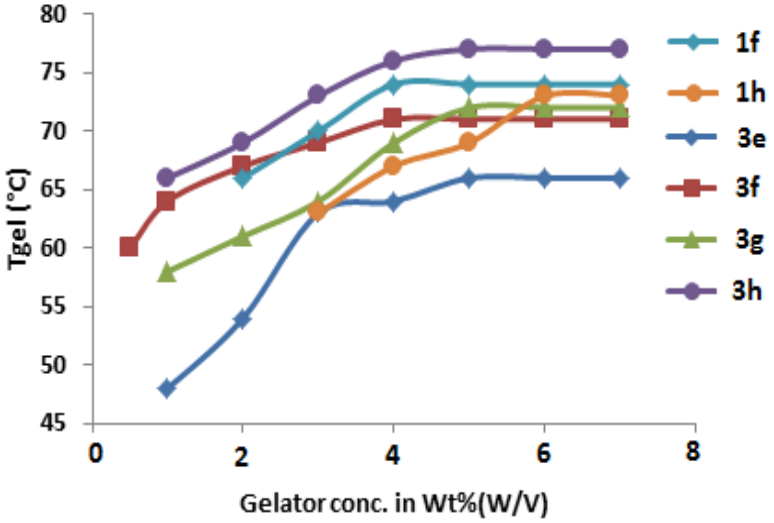

Figure 4.15 T_{gel} versus concentration plot of gel in methanol.

Understandably, the increase in concentration of gelator enhances the gel-to-sol transition temperature by actively participating in gelator fibres formation or by improving intermolecular interaction up to certain concentration. After reaching the critical concentration effect on the strength of gelator fibers and its interaction with gelling solvent, as represented by T_{gel} values, reaches a maximum value. The Tgel values of compounds 3e–3f before saturation demonstrated a gradual increase with the increase in the alkyl chain length, which supports the function of van der Waals interaction in enhancing the stability of the gel network. Furthermore, the gelators having an even number of methylene groups (3f and 3h) displayed higher value of gel–sol transition temperature than the gelators having an odd number of methylene groups (3e and 3g) in the alkyl chain as seen in Figure 4.15 at 4% wt.

A linear relationship obtained when semilog graph of the mole fraction of organogelators was plotted against $1/1000T_{gel}$ (K^{-1}) (**Figure 4.16)**, which agreed well with the Schroeder-van Laar equation (eq.1).

$$\ln[\text{gelator}] = -(\Delta H_m/RT_{gel}) + \text{constant} \quad \text{(eq. 1)}$$

Where, ΔH_m and T_{gel} are the enthalpy of melting and transition temperature of gel-to-sol, respectively. The gel-to-sol transition can be considered a first order transition assuming that the gel melts into an ideal solution and a known amount of gelator is involved in the transition.[24] From the plots, the enthalpy ΔH_m was calculated to be within the range of 71-192 kJ/mol. strikingly, enthalpy of melting of gel network (gel-sol transition) in the series **1e-1h** also showed odd even effect. ΔH_m of gel break down in the case of **3e** and **3g** (n=odd) found to have lower values than **3f** and **3h** (n=even) suggested the extra stability commanded by the gels of **3f** and **3h**.

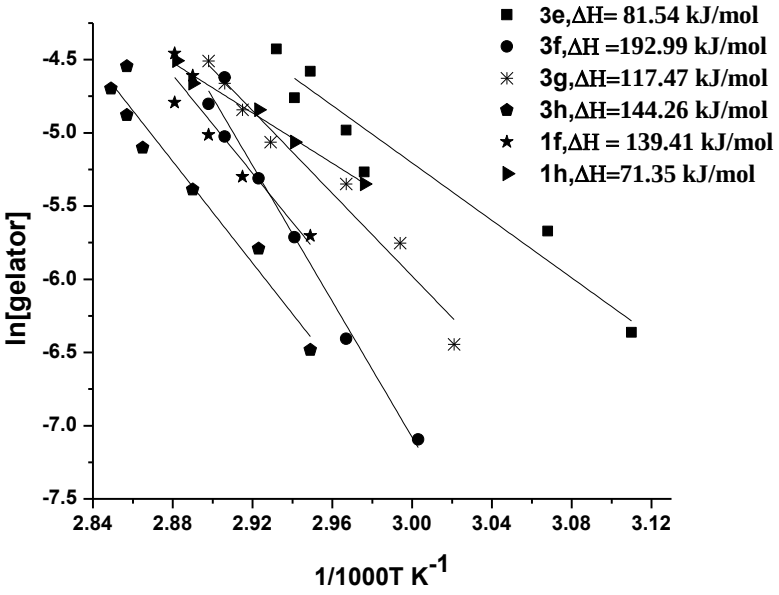

Figure 4.16 Semilog plot of the mole fraction of the gelators against 1/1000T (K^{-1}).

4.8.2 Morphological studies of xerogel

Scanning electron microscopy (SEM) micrographs were recorded for visualizing xerogels morphology derived from the gelators **1e**, **1h, 3b, 3c, 3e, 3f**, **3g** and **3h (Figure 4.17)**. Understandably, the solvent molecules are immobilized in 3-D network of fibers in the gel state. Dried gel networks of **1e** and **1h** displayed increased complexity of arrangement of gelator fibers with increase in methylene group and better entanglement of gelator fibers. The progressive increase in the entanglement of gelator fibers becomes more pronounced in the case of gelators (**3b**-**3h**).

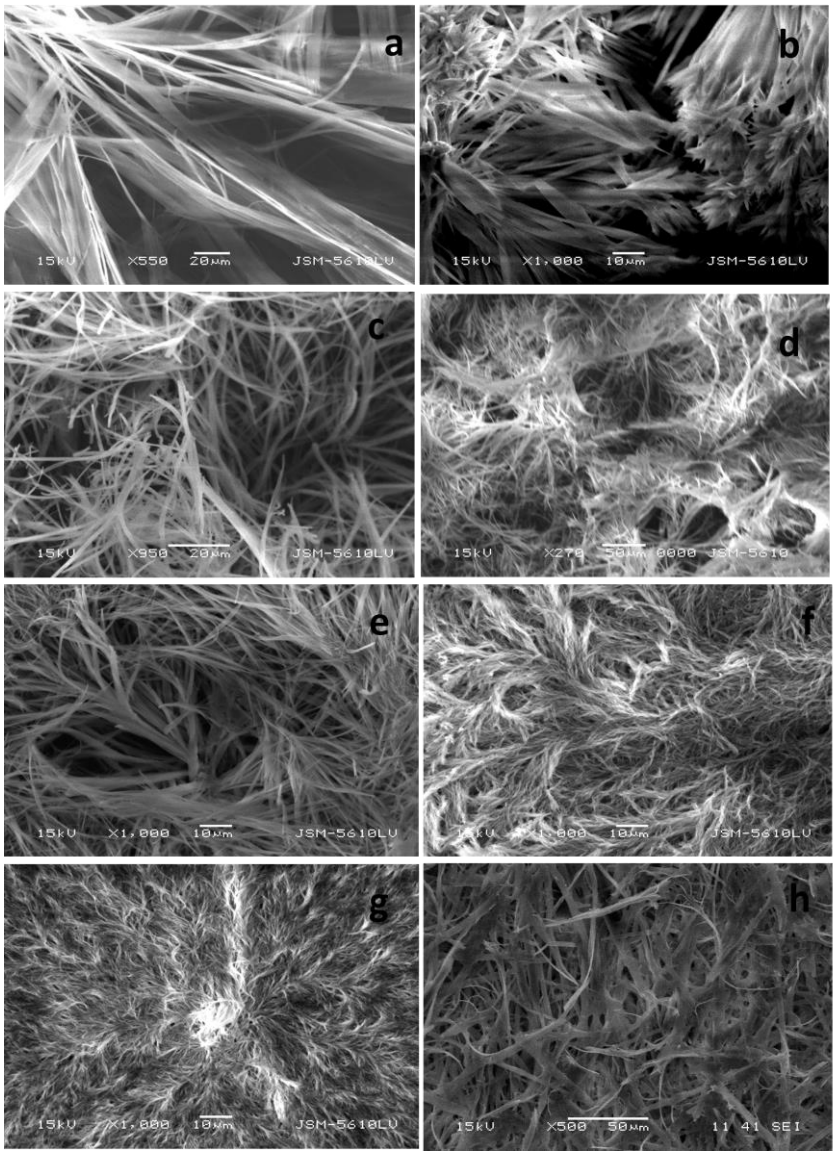

Figure 4.17 SEM images of xerogel of (a) 1e, (b) 1h (c) 3b (d)3c (e) 3e (f) 3f (g)3g and (h) 3h in methanol at 2 wt% (w/v).

A highly complex network of fibers is visible in the case of xerogel of **3h** with highly distinct pores, which may act as a reactor chamber of nanoparticles stabilized by gelators fibers.

4.8.3 Single crystal X-ray studies of 1b, 1c, 3b and 3c

Single crystals of **1b** were grown from methanol. Non-gelator **1b** showed a robust cyclic (amide) N-H...N (thiazole) supramolecular synthon leading to 0-D hydrogen bonded network along with O...S intramolecular interaction **(Fig.4.18a)**. Understandably, the non-gelling behaviour of **1b** can be attributed to the absence of one-dimensional hydrogen bonded network which presumably leads to fibre formation and, ultimately to immobilization of solvent. A suitable single crystal of gelator **1c** was obtained from choloroform having monoclinic ($P2_1/c$) space group. The asymmetric unit displayed a single molecule of **1c** joined together with another molecule through cyclic hydrogen bond N-H...N [N.... N = 2.942Å, ∟N-H...N = 173.21°] leading to the formation of the 0-D network. The 0-D network was extended to form the 2-D network through multiple C-H...O interaction **(Figure 4.18b)**. Single crystals of **3b** were grown from methanol. It was crystallized out in a space group Monoclinic P $2_1/c$. H-bonding pattern in the crystal seems to be governed by cyclic (amide)N-H...N (thiazole) synthons along with the intramolecular bond between carbonyl oxygen and thiazole sulphur atom, leading to a zero-dimensional (0-D) hydrogen bonded network. A critical examination of the crystal structures demonstrated a weaker hydrogen bond (methyl) C-H....N (thiazole) (distance between C...N= 3.535Å, ∟C-H...N = 147.7 °) leading to one-dimensional (1-D) hydrogen bonded network **(Figure 4.18c)**. **3c** crystallize out in a space group Triclinic P-1. H-bonding pattern in the crystal seems to be governed by cyclic (amide) N-H...N (thiazole) synthons[N.... N = 2.941Å, ∟N-H...N = 173.18°] along with the intramolecular bond between carbonyl oxygen and thiazole sulphur atom, leading to a zero-dimensional (0-D) hydrogen bonded network. A critical examination of the crystal structures demonstrated a weaker hydrogen bond (methyl) C-H....C (thiazole) (distance between C...C= 3.798Å, angle C-H...C= 160.67 °) and hydrogen bond (methyl) C-H....C (thiazole) (C....C= 3.394Å, ∟C-H...C= 82.47 ° leads to Two-dimensional (2-D) hydrogen bonded network **(Figure 4.18d) (**crystallographic parameters **Table 4.4)**.

One of the major challenges is to understand the cause of odd-even effect on gelation properties in these series of molecules. The urea functional group is known to favour anti or syn hydrogen bonded network leading to odd-even effect.[25] But no direct proof is available in amide based gelling systems to show such interaction. All the gelling/

non-gelling molecules in this series showed N-H...N hydrogen bonding between thiazole nitrogen and amide nitrogen instead of an amide-amide interaction **(Figure 4.11)**. Aakeroy et al.[26] seminal paper on competitive amide-amide interaction in comparison with other hydrogen bonded supramolecular synthons support our observation that amide-amide (0D or ladder type) interaction is less probable in presence of strong N-H...N H-bond. Interestingly, the C=O....S (intramolecular) forces found in all the crystal structures of thiazole amide, with or without a methyl functional group, appeared to force the long alkyl chain to be almost linear with respect to thiazole moiety. The linearity of alkyl chain seems to support interdigitation and helps in the formation of a weaker H-bond such as C-H....O, C-H...N, etc. Proximity of methyl group to alkyl chain disturbs the overall packing pattern and leads to 0-D dimensional hydrogen bonded network. Single crystal structures of **1b** (even, n=10) and **1c** (odd, n=11) highlighted additional C-H...O interaction in **1c** leading to 2-D hydrogen bonded network in comparison to **1b** which is a 0-D network.

A subtle odd-even effect was observed in the series of compounds **3b**-**3h** which showed an increase or decrease in mgc with one additional methylene group, which can be attributed to a suitable position of alkyl chain over one another and increasing interdigitation (n=even) along with additional C-H...O hydrogen bond. A pronounce effect of increase in alkyl chain length could be observed in the series of compounds **1a**-**1h** which displayed complete presence (n=even) or absence (n= odd) of gelation property. Structures reported displayed additional (methyl)C-H...O bond along with predominant C-H...N interaction with an increase in alkyl chain length from **3c** (n=10) to **3e** (n=12). We proposed interplay of weak interaction such as C-H...O, C-H...N as driving force for gelation in these series of compounds along with robust supramolecular synthons N-H...N, N-H...O interaction. A favourable presence of alkyl-alkyl chain interdigitation enhances the gelation properties and its absence in the supramolecular assembly of thiazole amides (**2a**-**2e**) loses its capability to immobilize any of the solvents used in the present study.

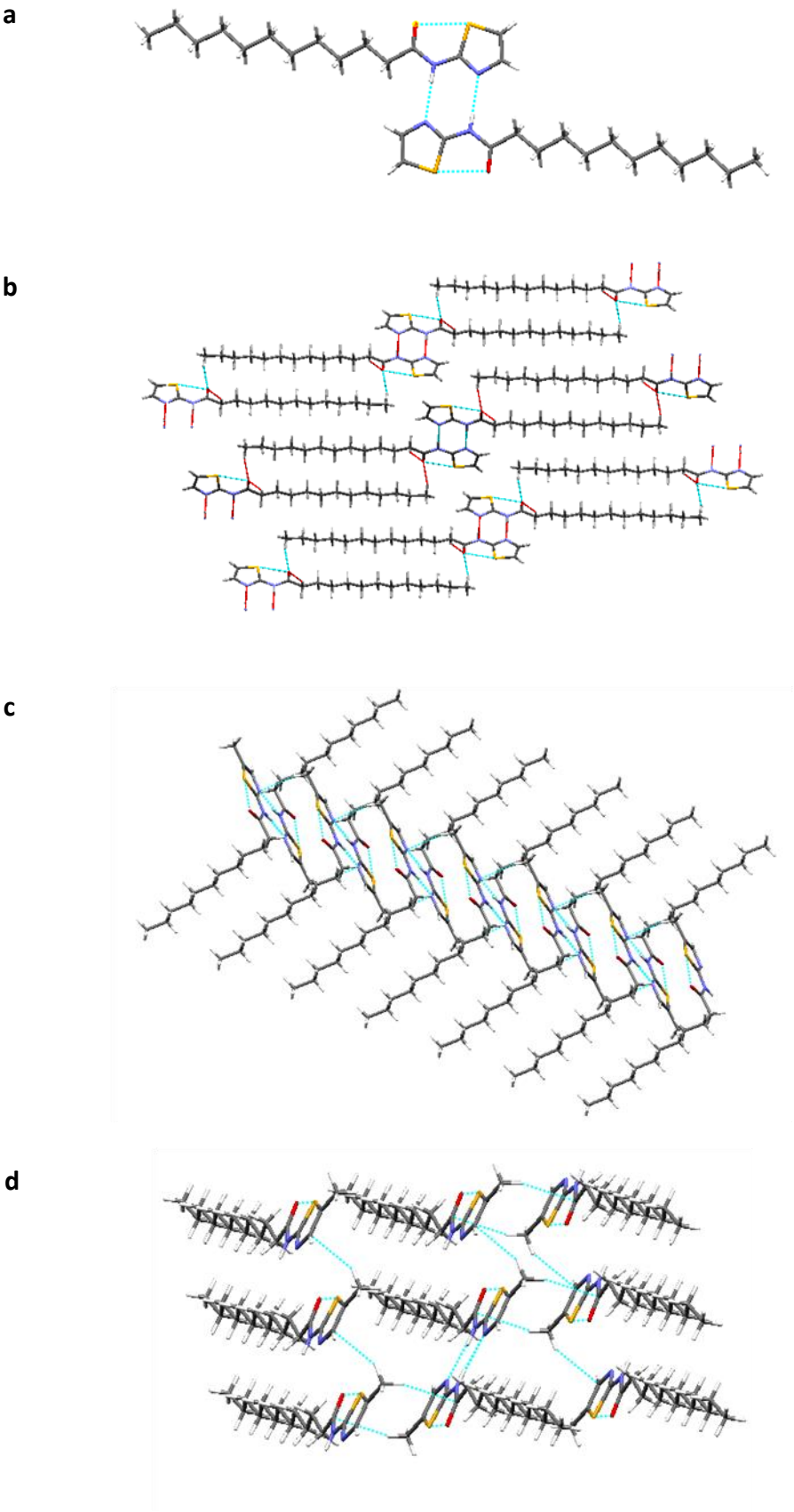

Figure 4.18 Hydrogen bonded network of (a) **1b** (b) **1c** (c) **3b** and (d) **3c.**

Table 4.4 Crystallographic parameters

	1b	1c	3b	3c
Empirical formula	C_{15} H_{26} N_2OS	$C_{32}H_{56}N_4O_2S_2$	C_{16} H_{28} N_2OS	C_{17} H_{30} N_2OS
Formula weight	282.44	296.47	296.46	310.51
Crystal size (mm)	0.3x 0.2 x 0.1	0.9x 0.15 x 0.15	0.32x 0.2 x 0.1	0.54x 0.45 x 0.15
Crystal system	Monoclinic	Monoclinic	Monoclinic	Triclinic
Space group	P 2_1/c	P 2_1/c	P 2_1/c	P-1
a/Å	20.8339(11)	20.6963(8)	20.0515(9)	4.9139(3)
b/Å	4.9640(3)	4.89895(19)	15.1825(9)	8.2041(5)
c/Å	15.5893(9)	16.9658(7)	5.5558(3)	23.1603(10)
α/°	90	90	90	84.043(4)
β/°	91.048(5)	97.371(4)	92.410(5)	87.033(4)
γ/°	90	90	90	78.743(5)
Volume/ $Å^{-3}$	1611.97(16)	1705.95(12)	1689.87(16)	910.32(9)
Z	4	1	4	2
D_{calc}	1.164	1.1543	1.165	1.1327
F(000)	616	648.71	648	341.5091
μ (mm^{-1})	0.197	1.154	0.191	1.575
Temperature (K)	293(2)	298	293(2)	293
Observed reflection *[I>2σ(I)]*	3155	3611	1954	3455
Parameters refined	173	192	183	191
Goodness of fit	1.070	1.1352	1.034	1.0861
Final R_1 on observed data	0.0569	0.0455	0.0637	0.0640
Final wR_2 on observed data	0.1449	0.1577	0.1206	0.1595
Source	Mo K_α	Mo K_α	Mo K_α	Cu K_α
Wavelength (Å)	0.7107	0.7107	0.7107	1.5418
CCDC No.	899103	958233	883759	965887

The powder X-ray diffraction (PXRD) study of xerogel of gelators/nongelators is frequently being carried out to get an insight into the packing of gelator fibers. PXRD of xerogel of gelling and non-gelling compounds with even/odd number of methylene functional group was recorded. **3b (n=12, even)** and **1d, 3d (n=14, even)** showed a periodical high intensity peak position in the lower 2θ angle in the ratio of 1:1/2: 1/3 suggesting lamellar packing such as 21.6034, 11.0243, 7.5231 for **1d**, 22.6578, 11.8392, 7.8609 for **3b** and 21.1379, 11.6241, 7.0921 for **3d (Figure 4.19)** .Whereas, in the case of **3c** and **1c (n=13,odd)** such periodical peaks were not observed. Based on these observation we can predict that alkyl –alkyl chain interdigitation might be the cause of odd-even effect on gelation properties.

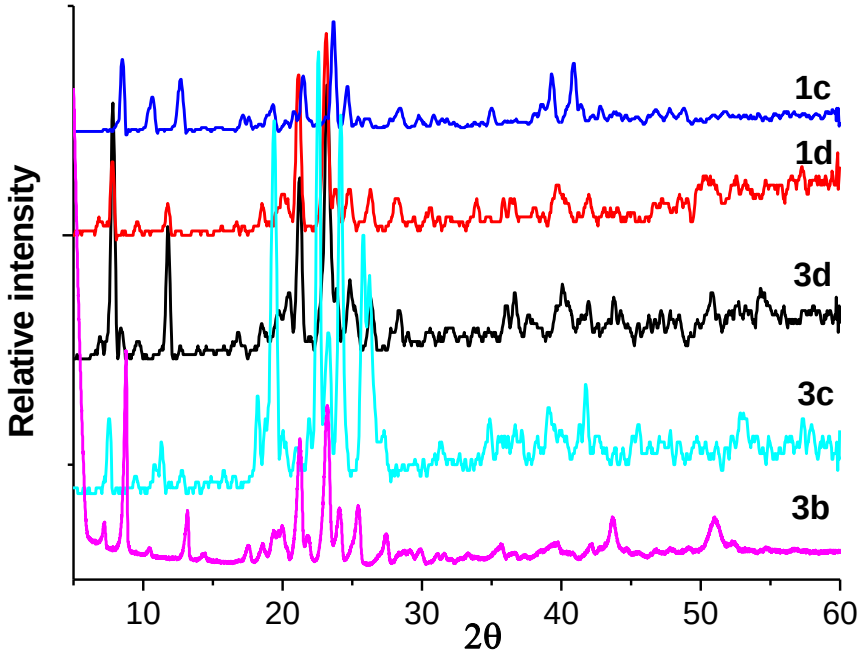

Figure 4.19 PXRD pattern of 1c-1d and 3b-3d.

4.8.4 Template directed synthesis of Ag and ZnO nanoparticles

ZnO nanoparticles loaded gelator samples were prepared by sol-gel method. Thermogravimetric analysis (TGA) of the sample was carried out to verify the removal of the gelator **(Figure 4.20)** from the synthesized ZnO nanoparticles. TGA analysis of the synthesized samples displayed weight loss of 74.4% corresponding to the complete removal of the gelator molecules at 350 °C.

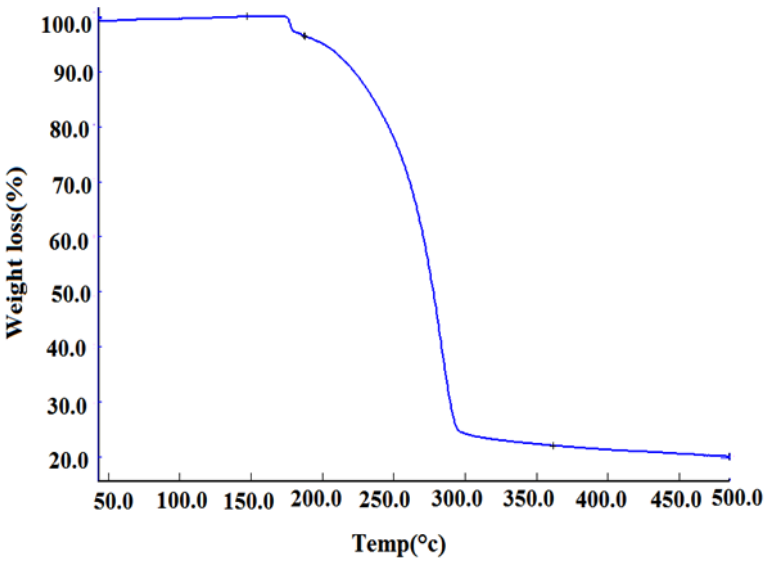

Figure 4.20 TGA curve for the Zno nanoparticles embedded in gelator.

The X-Ray diffraction pattern **(Figure 4.21 and 4.22)** provides further evidence for the formation silver and ZnO nano particles. The peaks were observed at diffraction angle 31, 39 and 45, corresponding to the (1 0 1),(1 1 1) and (2 0 0) crystalline planes of Ag, respectively**(Figure 4.21)**.[27] Similarly, the peaks were observed at diffraction angle 31, 36,47,56,62, and 67 corresponding to the (1 0 0),(1 0 1),(1 0 2),(1 1 0),(1 0 3) and (1 1 2) crystalline planes of ZnO, respectively**(Figure 4.22)**.[28]

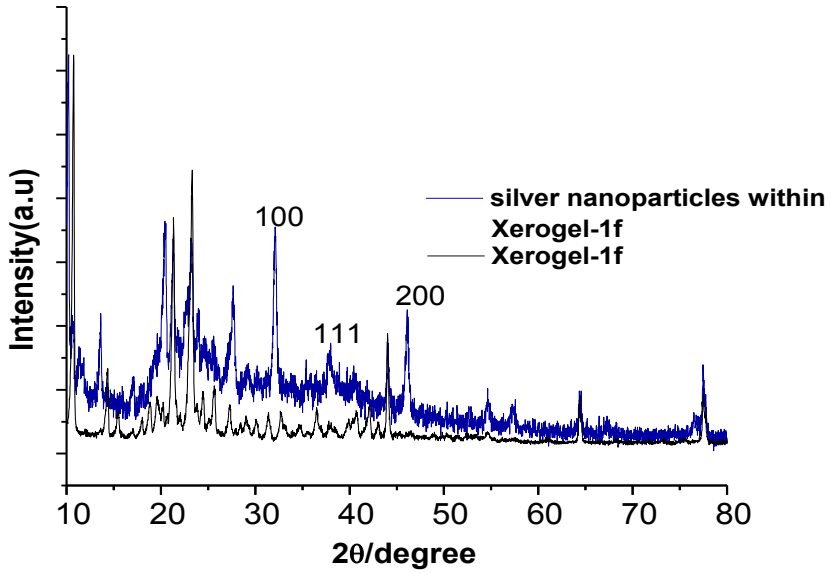

Figure 4.21 PXRD pattern of silver nanoparticles.

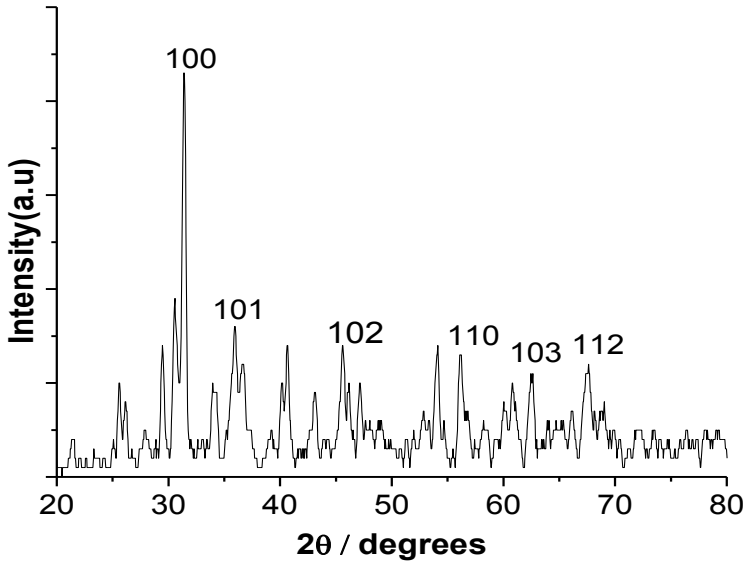

Figure 4.22 PXRD pattern of ZnO nanoparticles.

Transmission electron microscopy was used to characterize external morphology of the synthesized silver and ZnO nanoparticles. TEM imaging of Ag nanoparticles embedded in gel fibers (which acts as stabilizing and capping agent) was carried out **(Figure 4.23)**. Nearly spherical nanoparticles of Ag were observed in the TEM images suggested successful transcription of silver nanoparticles on of gelator fibers of **3b-3h**. The range of diameters of silver nanoparticles determined using TEM images of silver embedded in the gelled medium of **3b**, **3e**, **3f** and **3h** were found to increase with increase in the chain length **(Table 4.5)**. A progressive increase in the nanoparticles size with the increase in alkyl chain length suggested the probable increase in void between a 3-D network of gelator fibers. ZnO nanoparticles were subjected to TEM analysis after calcinations and complete removal of gelator template **(Figure 4.24)**.The range of diameters of the series of ZnO nanoparticles based on TEM images of **3b**,**3e**, **3f** and **3h** also followed the same trend of increase in size with increase of chain length **(Table 4.5)**.

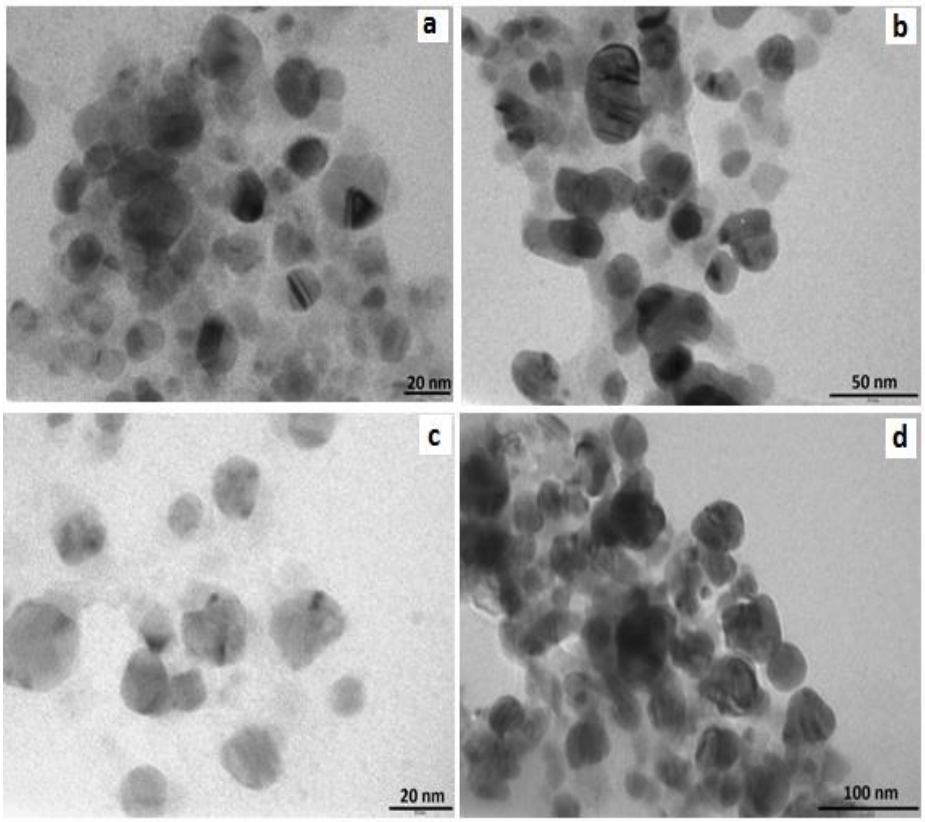

Figure 4.23 TEM images of silver nanoparticles formed within the gel network of (a) 3b (b) 3e (c) 3f (d) 3h.

Table 4.5 Particle Sizes of synthesized nanoparticles

	Range of diameter(nm) (Ag nanoparticle)	Range of diameter(nm) (ZnO nanoparticle)
3b(n=10)	5-20	10-20
3e(n=13)	18-30	20-30
3f(n=14)	25-37	24-40
3h(n=16)	30-50	28-52

The synthesized ZnO nanoparticles also displayed a gradual increase in size with one additional methylene functional groups change, which support the hypothesis that nanoparticles was synthesized in the well-defined void created by gelator fibers.

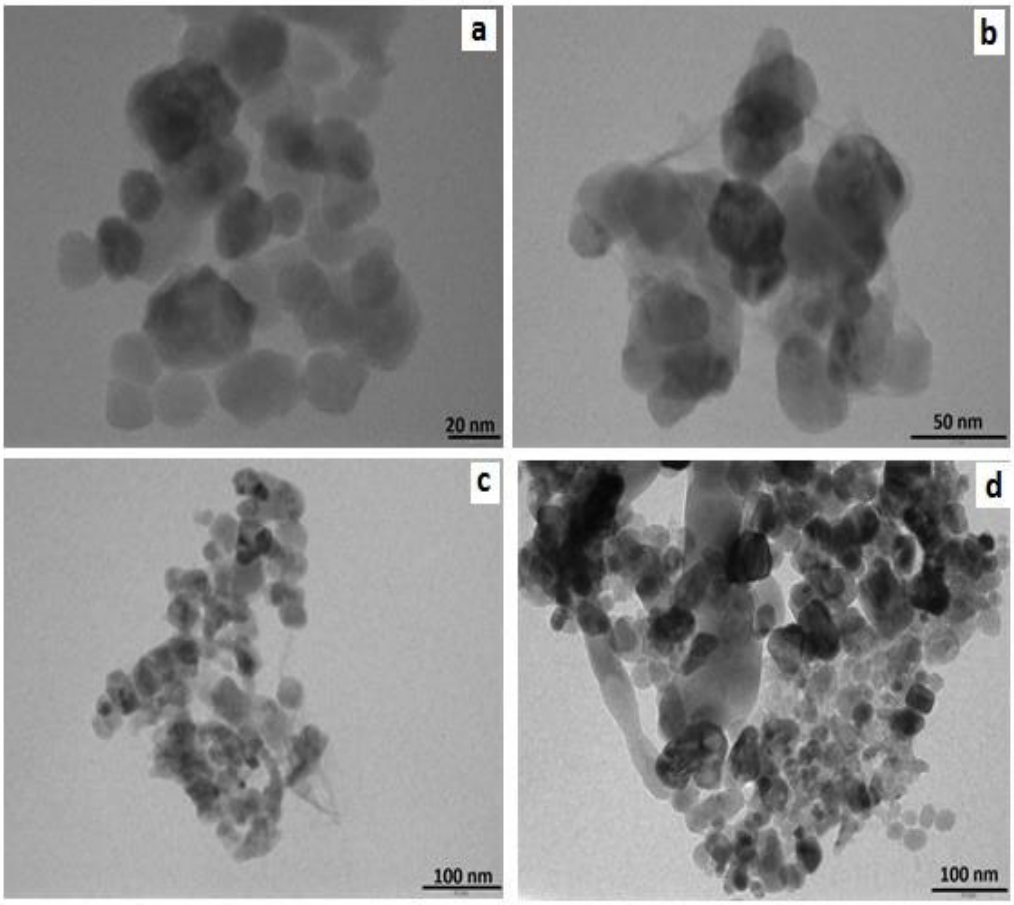

Figure 4.24 TEM image of ZnO nanoparticles formed within the gel network of (a)3b (b)3e (c)3f (d)3h.

A probable mechanism of nanoparticle synthesis is proposed in **Figure 4.25** based on single crystal studies of gelator/non-gelator and various physico-chemical analysis of thiazole based amide, and synthesized nano-particles.

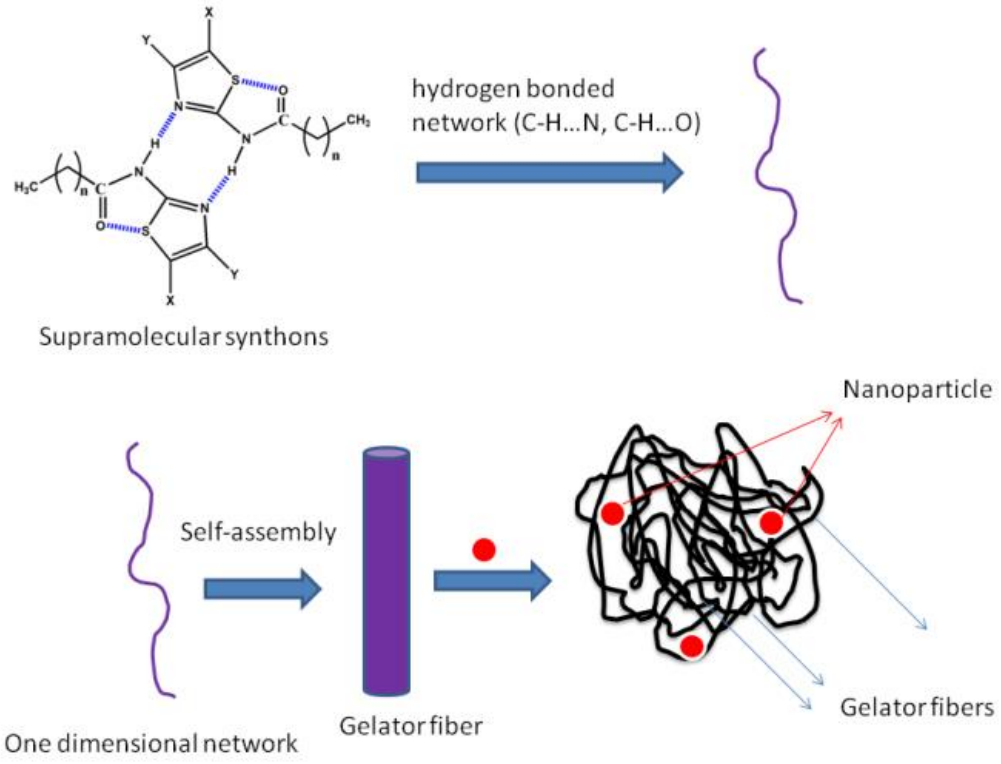

Figure 4.25 Proposed mechanism of template directed synthesis of nanoparticles in thiazole amide based gelator

4.8.5 Studies of silver nanoparticles embedded in gel network

Silver has long been known as an effective antimicrobial agent, for exhibiting strong toxicity to a wide range of micro-organisms. For this reason silver-based compounds and silver nanoparticles have been used extensively in many bactericidal applications.[29] One of the most important applications of silver and silver nanoparticles is in medical application such as topical ointments to prevent infection against burn and open wounds.[30] For this purpose a slow silver release rate is essential. Hence it is worth developing an antimicrobial gel formulation containing silver nanoparticles. Gelator composed of derivatives of amino thiazole, which is known for therapeutic application, along with embedded silver nanoparticles prompted us to explore the hybrid material as formulation of antimicrobial gel. In the present study, we have synthesized silver nanoparticles within the gel network, the solvent (ethanol) has been evaporated to get xerogel of compound 1f(C) which contain silver nanoparticles (N). To examine the bactericidal effect of silver nanoparticles on Gram-negative and gram positive bacteria, the colony of *E. coli* and

S.aurus were cultured on LB agar plates supplemented with compound 1f (C) and nanosized silver particles loaded within the gel fiber(N) **(Figure 4.26)**. The image depicts enhance antibacterial activity against *E.* coli and *S.aureus* in presence of silver nanoparticles adsorbed on gelator fibers(N). While compound 1f solely could not demonstrate any antibacterial activity (C). Organic-inorganic hybrid material such as 1f containing silver nanoparticles, may find potential application as good antimicrobial gel formulation.

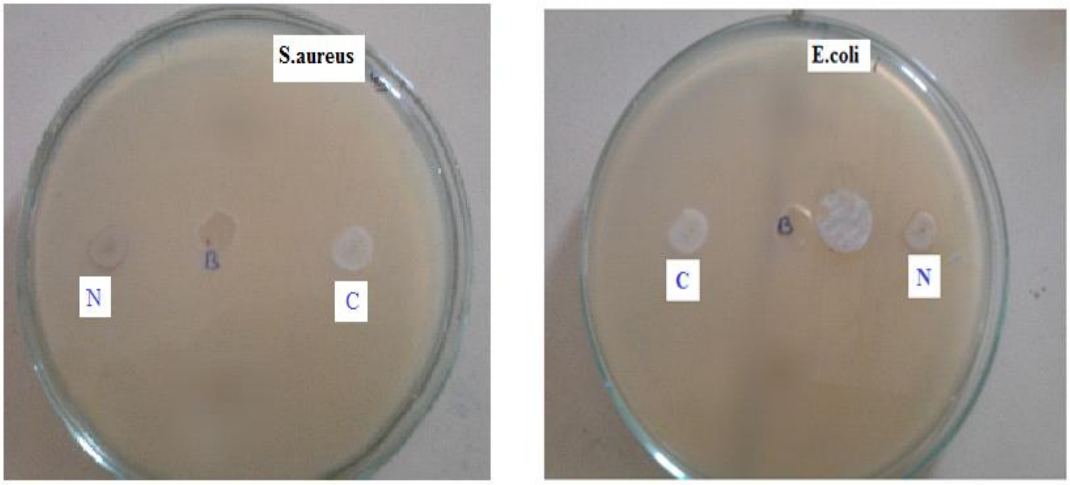

Figure 4.26 Images of antibacterial activities of 100 mg/l silver nanoparticles on Ecoli and S.aureus (N=silver nanoparticles, C=Compound 1f).

4.9 Conclusions

In the conclusion, we have synthesized and characterized new series of compounds **1a-1h**, **2a-2h** and **3a-3h** by systematically changing the alkyl chain length. A significant odd-even effect was observed in the series of compounds **1a-1h** and **3a-3h** beyond a certain critical chain length i.e. n=8 for **3 (3a)** and n=11 for **1 (1c).** This behaviour of gelling molecules was attributed to interplay between numerous hydrogen bonds such as C-H...O, C-H...N, etc. and van der Waals interaction between alkyl chains (interdigitation). The series of unsubstituted thiazole amide seems to induce gelation of organic solvents through a hydrogen bonded network supported by weak van der Waals interaction. The alkyl-alkyl chain interdigitation is conducive in the case of even number of methylene group which supported gelation whereas awkward packing of alkyl chain in the case of odd methylene groups of **1a-1h** leads to complete non-gelation behaviour. A less prominent odd-even effect of methylene group on organogelation properties of **3a-3h** may be attributed to the synergistic effect of (methyl)C-H...N(weak) and N-H...N(strong) H-bond capable of formation of 3-D network sufficient to immobilize a solvent in presence and/or absence of alkyl-alkyl interdigitation. A low cgc values and better efficiency of organgelators **3b-3h,** when 'n' is even, may be assigned to the extra stability by favourable alkyl-alkyl chain interaction. The present study establishes the weak H-bond (methyl) C-H...N as crucial interaction leading to 1-D network in 5-methylthiazole amide derivatives, whereas 4-methyl thiazole amide derivatives formed a 0-D network in absence of such interaction. Template directed synthesis of silver and ZnO nanoparticles were successfully carried out in gelators **3b-3h**. The size of nanoparticles of Ag and ZnO was found to be dependent on alkyl chain length of thiazole amides (**3b-3h**) suggested variation in the complexity of gelator network and tunability of pore size between fibers by a systematic increase in van der Waals interaction and interdigitation of alkyl chain. Silver nanoparticles embedded gel demonstrated the antimicrobial activity towards gram positive and gram negative bacteria, which propose its utility in slow silver release.

4.10 References

(1) X. Yu, L. Chen, M. Zhang, T. Yi, *Chem. Soc. Rev.*, **2014**,43,5346.

(2) J. W. Steed, *Chem. Soc. Rev*. **2010**, 39, 3686.

(3) L.Zhu, X.Li,S.Wu, K.T.Nguyen,H.Yan,H.Ågren,Y.Zhao, *J. Am. Chem. Soc*., **2013**, 135, 9174.

(4) F.Delbecq, K.Tsujimoto, Y.Ogue, H.Endo, T.Kawai, *J.Colloid Interface Sci*., **2013**,390,17.

(5)C.Morita, H.Tanuma,C.Kawai,Y. Ito, Y.Imura,T.Kawai, *Langmuir* ,**2013**, 29, 1669.

(6) F. Delbecq, K.Tsujimoto, Y. Ogue, T. Kawai, *Tetrahedron Lett*.,**2013**,54, 651.

(7)P.Xue, R.Lu, Y.Huang, M.Jin, C.Tan, C.Bao, Z.Wang, Y. Zhao, *Langmuir*,**2004**, 20, 6470.

(8) P.Gao, C.Zhan, M.Liu,*Langmuir*,**2006**, 22, 775.

(9) K.J.C.Van Bommel,A. Frigerri,S.Shinkai, *Angew.Chem.Int.Ed*., **2003**, 42, 980.

(10) M.Llusar,C. Sanchez, *Chem. Mater*., **2008**, 20, 782.

(11) P.Dastidar, *Chem.Soc.Rev*., **2008**, 37, 2699.

(12) A. Ballabh,T.K. Adalder, P. Dastidar, *Cryst. Growth & Des*., **2008**, 8, 4144.

(13)K. Aoki,M.Kudo,N.Tamaoki,*Org. Lett*., **2004**, 6, 4009.

(14)N.Fujita,Y. Sakamoto,M. Shirakawa,M. Ojima,A. Fujii,M. Ozaki,S.Shinkai, *J. Am.Chem. Soc*., **2007**, 129, 4134.

(15) Z.Fan,J.G. Lu, *J. Nanosci. Nanotech*., **2005**, 5, 1561.

(16) Q.Wan,C.L.Lin,X.B.Yu,T.H.Wang,*Appl. Phys. Lett.*, **2004**, 84, 124.

(17) A.Wei,X.W.Sun,C.X.Xu,Z.L.Dong,M.B. Yu,W. Huang, *Appl. Phys. Lett.*, **2006**, 88, 213102.

(18) M.George,R.G.Weiss,*Chem. Mater.*, **2003**, 15, 2879.

(19) Q.V.Dolomanov, L.B.Bourhis,R.J. Gildea,J.A.K. Howard,H. Puschmann, *J.Appl. Cryst*,. **2009**, 42, 339.

(20)G.M.Sheldrick,ActaCryst., **2008**, A64,112.

(21)G.Gundiah,S.Mukhopadhyay,U.G.Tumkurkar,A.Govindaraj,U.Maitra,C.N.R. Rao, *J. Mater. Chem.*,**2003**, 13, 2118.

(22)J.Cui,Y. Zheng,Z. Shen,X.Wan,*Langmuir*, **2010**, 26**,** 15508.

(23)N.Zweep,A.Hopkinson,A.Meetsma,W.R.Browne,B.L. Feringa, J.H.van Esch, *Langmuir*, **2009**, 25, 8802.

(24)U.K. Das,D.R. Trivedi,N.N. Adarsh,P. Dastidar, *J. Org. Chem*., **2009**, 74, 711.

(25)M.-O.M,Piepenbrock,G.O. Lloyd,N. Clarke,J.W. Steed,*Chem. Commun*., **2008**, 2644.

(26) C.B.Aakeröy,B.M.T.Scott,J.Desper, *New. J. Chem*., **2007**, 31, 2044.

(27)A.Mantion,A.G.Guex,A.Foelske,L.Mirolo,K.M.Fromm,M.Painsid,A.Taubert, *Soft Matter***, 2008**, 4, 606.

(28)L.Kumari,W.Z. Li,*Cryst. Res. Technol.*, **2010**, 45, 311.

(29)J.R.Morones,J.L.Elechiguerra,A.Camacho,K.Holt,J.B. Kouri,J.T.Ramirez, M.J. Yacaman, *Nanotechnology*, **2005**,16 , 2346.

(30)M.Ip,S.L. Lui,V.K.M. Poon,I. Lung,A. Burd, *J.Medical Microbiol*., **2006**, 55, 59.